Available online at www.sciencedirect.com
ScienceDirect
Journal of the Mechanics and Physics of Solids 56 (2008) 2494–2520
JOURNAL OF THE MECHANICS AND PHYSICS OF SOLIDS
www.elsevier.com/locate/jmps

Dynamics of a prestressed stiff layer on an elastic half space: filtering and band gap characteristics of periodic structural models derived from long-wave asymptotics

D. Bigoni[a,*], M. Gei[a], A.B. Movchan[b]

[a]*Department of Mechanical and Structural Engineering, University of Trento, Via Mesiano 77, I-38050 Trento, Italy*
[b]*Department of Mathematical Sciences, University of Liverpool, Liverpool L69 3BX, UK*

Received 10 August 2007; received in revised form 8 February 2008; accepted 24 February 2008

Abstract

Anti-plane and plane-strain, time-harmonic, small-amplitude vibrations of an elastic layer on an elastic half space are considered, superimposed upon a state of finite, uniform stress and strain. A (compressible) elastic material is considered, orthotropic with orthotropy axes aligned parallel and orthogonal both to the layer and the prestress principal directions. A non-uniform mass density is assumed in the layer. A formal long-wave asymptotic solution is derived under the assumptions of high contrast between the stiffnesses of the layer and the half space and between certain prestress components and the current elastic shear modulus.

It is shown that (i) the layer asymptotically behaves as a beam subject to transversal and axial vibrations; (ii) the response of the half space can be found in a closed-form, under the assumption of plane wave motion (which becomes consistent when the density of the layer is uniform), otherwise it is represented by a hypersingular integral equation; (iii) if the nonlocality introduced by the hypersingular integral equation is restricted to an influence area of finite extent, the integral can be analytically approximated, so that a Winkler-type spring model representing the half space is rigorously derived. For uniform density of the layer, the constants defining the spring model are given as functions of the prestress and anisotropy parameters of the half space; and, finally, (iv) the asymptotic solution provides new analytical expressions for incremental displacement of the layer, which, compared to the exact numerical solution (also included), are shown to perform quite well, even for values of parameters much beyond the limits imposed by the asymptotic analysis.

The asymptotic analysis allows us to explore, for the first time, dynamic properties of a periodic layer bonded to an elastic half space and subject to a uniform prestress state. We find that the system exhibits band gaps (ranges of forbidden frequencies) and that the prestress can be used as a parameter tuning the filtering properties of the structure, an effect which may have important consequences in the design of resonant devices.

Keywords: Elastic waves; Prestressed materials; Band gaps; Periodic structures; Asymptotic analysis

*Corresponding author. Tel.: +39 0461 882507; fax: +39 0461 882599.
E-mail addresses: bigoni@ing.unitn.it (D. Bigoni), mgei@ing.unitn.it (M. Gei), abm@liv.ac.uk (A.B. Movchan).

0022-5096/$ - see front matter © 2008 Elsevier Ltd. All rights reserved.
doi:10.1016/j.jmps.2008.02.007

1. Introduction

An anisotropic, prestressed elastic layer on an elastic half space is a model finding a broad range of applications, including: the Earth's crust in seismology, the foundation/soil interaction in geotechnical engineering, tissue structures in biomechanics, coated solids in material science, and micro-electro-mechanical systems (MEMS).

In all these situations (even in tissue biomechanics, Zamir and Taber, 2004, and MEMS, Cimpoiasu et al., 1996; Lian and Sottos, 2004), the presence of a prestress strongly influences results, particularly the dynamic behaviour,[1] so that prestress analysed within the framework of incremental nonlinear elasticity is the focus of a number of studies (among others: Bigoni et al., 1997; Cai and Fu, 2000; Gei, 2008; Gei and Ogden, 2002; Gei et al., 2004; Gurtin and Murdoch, 1975; Ogden and Steigmann, 2002; Steigmann and Ogden, 1997, 1999). In particular, Gurtin and Murdoch (1975) formulated a simplified theory in which the layer becomes a membrane, while a bending stiffness has been introduced in this membrane model by Steigmann and Ogden (1997, 1999). However, 'membrane models' are purely phenomenological, in the sense that the characteristics of the coating are not derived, rather postulated. The only available asymptotic derivation of these characteristics has been given by Cai and Fu (2000), under the assumptions of quasi-static incremental deformations and homogeneous layer.

The aims of the present paper are:

- To formulate a model for an orthotropic, prestressed (compressible) elastic layer vibrating on an elastic half space. The following assumptions are introduced: time-harmonic motion; directions of orthotropy coincident with the principal directions of prestress and aligned parallel and orthogonal with the layer surface; elastic half space of negligible inertia and small stiffness. The elastic laws are chosen in full generality and *the density of the layer is possibly nonuniform*. Both anti-plane and plane-strain incremental deformations, superimposed to the given uniform state of prestress, are considered.
- To derive — in the framework of asymptotic theory of elasticity — a structural model of the above mechanical continuous system. This is obtained under the long-wave approximation and the hypothesis of high contrast between the stiffnesses of the layer and of the half space and between certain prestress components. It is shown that the layer behaves as a beam subject to longitudinal and transversal time-harmonic vibrations and that, in the most general case, the half space interacts with the layer through a hypersingular integral in an integro-differential equation.
- To show that the hypersingular integral representing the response of the half space can be rigorously reduced to a spring-like, so-called 'Winkler', model in two relevant cases, namely, when (i) the layer is uniform (so that the vibrations can be resolved into planar waves); and (ii) a 'cut-off' in the interaction zone between layer and half space is introduced. This cut-off, inspired from analogous interaction lengths employed in molecular-dynamics simulations, is explicitly evaluated when the layer is uniform and leads to simple formulae for the stiffness of the spring-like model, which include the effects of prestress and material orthotropy.
- To provide a new asymptotic closed-form formulae solving both anti-plane and plane-strain harmonic vibrations of a homogeneous layer and to compare these solutions with exact solutions (also included), requiring numerical solution of a characteristic equation. The comparison shows such an excellent behaviour of the asymptotic formulae that these remain valid even when the hypotheses on the basis of the asymptotic solution (high contrast between the two media stiffnesses and negligible mass density of the substrate) are clearly violated.

The most interesting possibility which is open by the above results is to analyse the case of a hard prestressed layer with periodic properties, bonded to a soft elastic substrate, a typical configuration of devices employed in the field of 'flexible electronics', where thin gold conductors are deposited on polydimethylsiloxane (PDMS) substrates to ensure high 'global' deformability of the system (Gray et al., 2004; Li et al., 2004).

[1]The fact that compressive (tensile) axial load lowers (increases) the natural frequencies of beams subject to flexural vibrations and of much more complicated structures is well understood in structural engineering (see Mead, 2002, and references quoted therein) and similar conclusions can be reached in two-dimensional boundary-value problems of prestressed solids (Bigoni et al., 2007).

The density ratio between the two materials is about $\frac{1}{20}$, while the stiffness ratio is about 1 MPa/78 000 MPa, values that certainly satisfy our asymptotic smallness requirements.

In particular, we analyse the case of a *periodic, piecewise constant density distribution of the prestressed layer*, which allows an explicit analysis via the Floquet–Bloch technique (Bigoni and Movchan, 2002; Platts et al., 2003; Guenneau and Movchan, 2004). This analysis reveals that the system (as usual in periodic structures) exhibits band gaps (i.e. ranges of forbidden frequencies), but *we show a new important effect*, *namely*, *that the prestress influences* (*in a sense* '*shifts*') *the band gaps/pass bands*, so that we conclude that the prestress can be used as a 'tuning' parameter to change the filtering properties of the system, a finding which may have applications in the design of resonant MEMS.

2. Elastic material with prestress

We refer to an elastic material uniformly stressed and stretched (possibly orthotropic, but with orthotropy axes aligned with the principal directions of stress and stretch), so that the Cauchy stress $\boldsymbol{\sigma}$ and the left stretch tensor $\boldsymbol{V}$ are coaxial and represented by

$$\boldsymbol{\sigma} = \sigma_1 \boldsymbol{K}_1 + \sigma_2 \boldsymbol{K}_2 + \sigma_3 \boldsymbol{K}_3, \quad \boldsymbol{V} = \lambda_1 \boldsymbol{K}_1 + \lambda_2 \boldsymbol{K}_2 + \lambda_3 \boldsymbol{K}_3, \tag{1}$$

where σ_i and λ_i $(i = 1, 2, 3)$ are the principal values of Cauchy stress and the principal stretches, respectively, and

$$\boldsymbol{K}_i = \boldsymbol{k}_i \otimes \boldsymbol{k}_i \quad (i = 1, 2, 3) \tag{2}$$

are the dyads collecting the unit eigenvectors common to $\boldsymbol{\sigma}$ and $\boldsymbol{V}$, so that $\{\boldsymbol{k}_1, \boldsymbol{k}_2, \boldsymbol{k}_3\}$ is the orthonormal triad defining the principal directions of stress, stretch and orthotropy. In this paper, we assume that the directions singled out by unit vectors $\boldsymbol{k}_i$ $(i = 1, 2, 3)$ are (spatial) directions of *orthotropy existing independently of the prestress* (so that they remain defined also in the absence of prestress or when the prestress is isotropic).

It is expedient now to employ the (symmetric) Kirchhoff stress $\boldsymbol{K}$, defined in terms of Cauchy stress $\boldsymbol{\sigma}$ as

$$\boldsymbol{K} = J\boldsymbol{\sigma} = \kappa_1 \boldsymbol{K}_1 + \kappa_2 \boldsymbol{K}_2 + \kappa_3 \boldsymbol{K}_3,$$

where J denotes the determinant of the deformation gradient and $\kappa_i = J\sigma_i$ $(i = 1, 2, 3)$ the eigenvalues of the Kirchhoff stress. An arbitrary objective flux (for instance the Jaumann or Oldroyd or convected fluxes can be employed) of Kirchhoff stress is assumed to be derivable from an incremental energy function ψ defined in such a way that

$$\overset{\circ}{\boldsymbol{K}} = \frac{\partial \psi(\boldsymbol{D}, \boldsymbol{K}_1, \boldsymbol{K}_2)}{\partial \boldsymbol{D}}. \tag{3}$$

The function ψ is a scalar isotropic function of its tensorial arguments: the Eulerian incremental strain tensor $\boldsymbol{D}$ and the dyads singling out the principal stress directions ($\boldsymbol{k}_3 \otimes \boldsymbol{k}_3$ is not made explicit since it can be expressed as $\boldsymbol{I} - \boldsymbol{k}_1 \otimes \boldsymbol{k}_1 - \boldsymbol{k}_2 \otimes \boldsymbol{k}_2$). Representation theorems of isotropic functions (Wang, 1970) show that, for linear incremental response, the incremental potential can be expressed as

$$\begin{aligned}\psi = {} & \frac{e_1}{2}(\boldsymbol{k}_1 \cdot \boldsymbol{D}\boldsymbol{k}_1)^2 + \frac{e_2}{2}(\boldsymbol{k}_2 \cdot \boldsymbol{D}\boldsymbol{k}_2)^2 + \frac{e_3}{2}(\boldsymbol{k}_3 \cdot \boldsymbol{D}\boldsymbol{k}_3)^2 + e_4(\boldsymbol{k}_1 \cdot \boldsymbol{D}\boldsymbol{k}_1)(\boldsymbol{k}_2 \cdot \boldsymbol{D}\boldsymbol{k}_2) \\ & + e_5(\boldsymbol{k}_1 \cdot \boldsymbol{D}\boldsymbol{k}_1)(\boldsymbol{k}_3 \cdot \boldsymbol{D}\boldsymbol{k}_3) + e_6(\boldsymbol{k}_2 \cdot \boldsymbol{D}\boldsymbol{k}_2)(\boldsymbol{k}_3 \cdot \boldsymbol{D}\boldsymbol{k}_3) + e_7(\boldsymbol{k}_1 \cdot \boldsymbol{D}^2\boldsymbol{k}_1) + e_8(\boldsymbol{k}_2 \cdot \boldsymbol{D}^2\boldsymbol{k}_2) + e_9(\boldsymbol{k}_3 \cdot \boldsymbol{D}^2\boldsymbol{k}_3),\end{aligned} \tag{4}$$

where the nine coefficients e_j $(j = 1, \ldots, 9)$ are arbitrary functions of the principal values of (Cauchy) prestress σ_i and/or prestretch λ_i. Note that in Eq. (4) we have reintroduced $\boldsymbol{k}_3 \otimes \boldsymbol{k}_3$ to make explicit the equal influence of the three principal stress axes.

The fourth-order incremental elastic tensor, possessing both minor and major symmetries, and relating the selected objective derivative of the Kirchhoff stress to the Eulerian strain increment, that is,

$$\overset{\circ}{\boldsymbol{K}} = \mathbb{E}[\boldsymbol{D}], \tag{5}$$

can be obtained from Eq. (3) as

$$\begin{aligned}\mathbb{E} = {} & e_1\boldsymbol{K}_1\otimes\boldsymbol{K}_1 + e_2\boldsymbol{K}_2\otimes\boldsymbol{K}_2 + e_3\boldsymbol{K}_3\otimes\boldsymbol{K}_3 + e_4(\boldsymbol{K}_1\otimes\boldsymbol{K}_2 + \boldsymbol{K}_2\otimes\boldsymbol{K}_1)\\ & + e_5(\boldsymbol{K}_1\otimes\boldsymbol{K}_3 + \boldsymbol{K}_3\otimes\boldsymbol{K}_1) + e_6(\boldsymbol{K}_2\otimes\boldsymbol{K}_3 + \boldsymbol{K}_3\otimes\boldsymbol{K}_2)\\ & + e_7(\boldsymbol{I}\,\underline{\otimes}\,\boldsymbol{K}_1 + \boldsymbol{K}_1\,\underline{\otimes}\,\boldsymbol{I}) + e_8(\boldsymbol{I}\,\underline{\otimes}\,\boldsymbol{K}_2 + \boldsymbol{K}_2\,\underline{\otimes}\,\boldsymbol{I}) + e_9(\boldsymbol{I}\,\underline{\otimes}\,\boldsymbol{K}_3 + \boldsymbol{K}_3\,\underline{\otimes}\,\boldsymbol{I}),\end{aligned} \tag{6}$$

where the following two tensorial products between second-order tensors $\boldsymbol{A}$, $\boldsymbol{B}$ and $\boldsymbol{C}$ have been used

$$(\boldsymbol{A}\otimes\boldsymbol{B})[\boldsymbol{C}] = (\boldsymbol{B}\cdot\boldsymbol{C})\boldsymbol{A}, \quad (\mathbf{A}\,\underline{\otimes}\,\mathbf{B})[\mathbf{C}] = \tfrac{1}{2}(\mathbf{A}\mathbf{C}\mathbf{B}^{\mathrm{T}} + \mathbf{A}\mathbf{C}^{\mathrm{T}}\mathbf{B}^{\mathrm{T}}). \tag{7}$$

Note that the elastic isotropic fourth-order tensor of linear elasticity, defined by the two Lamé constants λ and μ, is recovered from Eq. (6) by taking

$$e_1 = e_2 = e_3 = e_4 = e_5 = e_6 = \lambda, \quad e_7 = e_8 = e_9 = \mu. \tag{8}$$

It is clear from Eq. (6) that the incremental response of a prestressed material is always orthotropic (even when the material is initially isotropic, if prestressed) and depends upon nine independent coefficients, arbitrary functions of the current principal values of prestress $\{\sigma_1, \sigma_2, \sigma_3\}$ and/or prestretch $\{\lambda_1, \lambda_2, \lambda_3\}$.

Identifying the objective increment of Kirchhoff stress with the Jaumann increment and employing a relative Lagrangean description in which the current configuration is assumed as the reference configuration, the deformation gradient becomes the identity and $J = 1$, so that the increment of the nominal (the transpose of the first Piola–Kirchhoff) stress $\boldsymbol{t}$ is related to the Jaumann increment of the Kirchhoff stress through

$$\dot{\boldsymbol{t}} = \overset{\triangledown}{\boldsymbol{K}} - \boldsymbol{K}\boldsymbol{W} - \boldsymbol{D}\boldsymbol{K}, \tag{9}$$

where $\boldsymbol{W}$ is the incremental rotation tensor, so that the displacement incremental gradient $\boldsymbol{L}$ is defined as $\boldsymbol{L} = \boldsymbol{D} + \boldsymbol{W}$. Employing Eqs. (6) and (9) the constitutive equation can be expressed in the form $\dot{\boldsymbol{t}} = \mathbb{C}[\boldsymbol{L}]$, where

$$\mathbb{C} = \mathbb{E} + \mathbb{G} - \boldsymbol{I}\,\underline{\otimes}\,\boldsymbol{K} + \boldsymbol{K}\,\underline{\otimes}\,\boldsymbol{I} - \boldsymbol{K}\boxtimes\boldsymbol{I}, \tag{10}$$

in which, for every tensor $\boldsymbol{A}$, $\boldsymbol{B}$ and $\boldsymbol{C}$, $(\boldsymbol{A}\boxtimes\boldsymbol{B})[\boldsymbol{C}] = \boldsymbol{A}\boldsymbol{C}\boldsymbol{B}^{\mathrm{T}}$, so that $\mathbb{C}$ still retains the major symmetry of $\mathbb{E}$, but looses the minors.

It is worth noting that the incremental equations of small-amplitude vibrations superimposed upon a given uniform state (of strain and stress) in the absence of body forces can be written as

$$\dot{t}_{ji,j} = \rho u_{i,tt}, \tag{11}$$

where ρ is the mass density in the current configuration (assumed as reference), u_j is the incremental displacement and t denotes the time variable.

Two special cases of constitutive Eqs. (10) will be addressed in this paper, namely, the particularizations pertaining to incremental anti-plane shearing and plane strain. These are considered below.

2.1. Incremental anti-plane shearing

For anti-plane shearing, the incremental displacement takes the form

$$v_1 = v_2 = 0, \quad v_3 = v_3(x_1, x_2),$$

so that the non-null components of the Eulerian incremental strain and spin are

$$D_{13} = D_{31} = -W_{13} = W_{31} = \frac{v_{3,1}}{2}, \quad D_{23} = D_{32} = -W_{23} = W_{32} = \frac{v_{3,2}}{2}.$$

Assuming that the Cauchy prestress has principal components σ_1, σ_2, σ_3, the constitutive response reduces to the only non-null nominal stress increments

$$\dot{t}_{31} = \left(\mu - \frac{\sigma_1}{2}\right)v_{3,1}, \quad \dot{t}_{13} = \left(\mu + \frac{\sigma_1}{2}\right)v_{3,1}, \quad \dot{t}_{32} = \left(\mu - \frac{\sigma_2}{2}\right)v_{3,2}, \quad \dot{t}_{23} = \left(\mu + \frac{\sigma_2}{2}\right)v_{3,2}, \tag{12}$$

where

$$\mu = \frac{e_7 + e_9 - \sigma_3}{2},$$

so that symmetry is recovered in the special case $\sigma_1 = \sigma_2 = 0$.

Substituting Eqs. (12) into Eqs. (11), we derive the equation of motion in the presence of prestress for anti-plane shearing

$$\mu_1 v_{3,11} + \mu_2 v_{3,22} = \rho v_{3,tt}, \tag{13}$$

where the two moduli

$$\mu_1 = \mu + \frac{\sigma_1}{2}, \quad \mu_2 = \mu + \frac{\sigma_2}{2}$$

have been introduced to simplify notation.

2.2. Incremental plane-strain deformation

For plane-strain incremental deformations (denoting with index 3 the out-of-plane direction), we have

$$D_{i3} = D_{3i} = W_{i3} = -W_{3i} = 0 \quad (i = 1, 2, 3),$$

so that Eqs. (5) and (6) give the following non-null in-plane components:

$$\overset{\nabla}{K}_{11} = (e_1 + 2e_7)D_{11} + e_4 D_{22}, \quad \overset{\nabla}{K}_{22} = e_4 D_{11} + (e_2 + 2e_8)D_{22}, \quad \overset{\nabla}{K}_{12} = \overset{\nabla}{K}_{21} = (e_7 + e_8)D_{12}, \tag{14}$$

plus the out-of-plane component

$$\overset{\nabla}{K}_{33} = (e_3 + 2e_9)D_{33} + e_5 D_{11} + e_6 D_{22}. \tag{15}$$

In terms of nominal stress increment, the constitutive equations (9) yield for the in-plane components[2]

$$\dot{t}_{11} = a v_{1,1} + c v_{2,2}, \quad \dot{t}_{22} = b\, v_{2,2} + c v_{1,1}, \quad \dot{t}_{12} = \alpha v_{2,1} + \gamma v_{1,2}, \quad \dot{t}_{21} = \gamma v_{2,1} + \beta v_{1,2}, \tag{16}$$

where the notation used by Hill (1979)[3] has been introduced:

$$a = e_1 + 2e_7 - \sigma_1, \quad b = e_2 + 2e_8 - \sigma_2, \quad c = e_4,$$
$$\left.\begin{matrix}\alpha \\ \beta\end{matrix}\right\} = \frac{e_7 + e_8}{2} \pm \frac{\sigma_1 - \sigma_2}{2}, \quad \gamma = \frac{e_7 + e_8}{2} - \frac{\sigma_1 + \sigma_2}{2}. \tag{17}$$

Substituting Eqs. (16) into Eq. (11), we obtain the equations of plane-strain motion in the presence of prestress

$$a v_{1,11} + c v_{2,12} + \gamma v_{2,12} + \beta v_{1,22} = \rho v_{1,tt}, \quad \alpha v_{2,11} + \gamma v_{1,21} + c v_{1,12} + b v_{2,22} = \rho v_{2,tt}. \tag{18}$$

On the basis of Eqs. (18) Hill (1979) has given the ellipticity condition

$$|ab + \alpha\beta - (c + \gamma)^2| < 2\sqrt{ab\alpha\beta}, \quad ab\alpha\beta > 0,$$

to which calculations performed in this paper are restricted.

3. Anti-plane small-amplitude vibrations of a prestressed layer on a half space

Consider an elastic thin layer of thickness εh, where ε is a small non-dimensional parameter ($0 < \varepsilon \ll 1$) and h is a length scale, subject to dead loading on the upper boundary Θ and resting on a much less stiff elastic half

[2]The out-of-plane component of nominal stress increment coincides with the homologous component of the Jaumann derivative, Eq. (15).

[3]Hill (1979, his Eqs. (2.1)) writes Eq. (14) in terms of Jaumann derivative of Cauchy stress, instead of Kirchhoff stress. The equivalence of the two notations becomes evident when the formulae written in terms of nominal stress increment, his Eqs. (2.7), are compared to our Eqs. (16) and (17).

space. Let us fix a cartesian coordinate system such that the interface Γ between layer and half space coincides with the plane x_1–x_3 and the axis x_2 is directed toward the upper boundary Θ. We assume that the two media follow the constitutive law (12) with orthotropy in the layer induced by prestress.

The substrate is taken to be isotropic with incremental shear stiffness μ^s much smaller than that of the layer, so that Eqs. (12) become

$$\dot{t}^s_{31} = \dot{t}^s_{13} = \varepsilon^\zeta \bar{\mu}^s v^s_{3,1}, \quad \dot{t}^s_{32} = \dot{t}^s_{23} = \varepsilon^\zeta \bar{\mu}^s v^s_{3,2},$$

where the superscript s denotes quantities associated with the half space, $\zeta > 0$ and $\bar{\mu}^s$ is of the same order as μ_1, μ_2.

We study the case of propagation of a shear wave along the x_2-axis with only nonvanishing component of the displacement vector u along the x_3-axis. For isotropic elasticity without prestress, this is the so-called 'Love wave problem', which admits solution only if the propagation speed of shear waves in the layer is smaller than the propagation speed in the half space (a condition that is always satisfied here since the half space will be assumed to have a negligibly small mass density).

Limiting the analysis to time-harmonic oscillations with circular frequency ω for the layer, the equation of motion (13) takes the form

$$\mu_1 \frac{\partial^2 u}{\partial x_1^2} + \mu_2 \frac{\partial^2 u}{\partial x_2^2} + \rho(x_1, x_2)\omega^2 u = 0, \tag{19}$$

where $u = v_3$, while for the half space

$$\varepsilon^\zeta \bar{\mu}^s \left(\frac{\partial^2 u^s}{\partial x_1^2} + \frac{\partial^2 u^s}{\partial x_2^2} \right) + \rho^s \omega^2 u^s = 0, \tag{20}$$

which is assumed to possess a negligibly small mass density (an assumption that is justified in several contexts, for instance, the mass density ratio can be $\frac{1}{5}$ for a steel beam on a gravel substrate and can fall to $\frac{1}{10}$ for a wooden substrate and to $\frac{1}{20}$ in the case mentioned in the Introduction of a thin gold conductor over a PDMS substrate), $\rho^s = 0$. The boundary conditions for the layer are:

- null incremental nominal tractions at the upper boundary Θ of the layer (which is subjected to dead loading)

$$\left. \frac{\partial u}{\partial x_2} \right|_\Theta = 0; \tag{21}$$

- continuity of nominal traction and displacement increments across the interface Γ between layer and half space

$$\varepsilon^\zeta \bar{\mu}^s \left. \frac{\partial u^s}{\partial x_2} \right|_\Gamma = \mu_2 \left. \frac{\partial u}{\partial x_2} \right|_\Gamma, \quad u^s|_\Gamma = u|_\Gamma. \tag{22}$$

In the layer we introduce now the scaled variable

$$\xi = \frac{x_2}{\varepsilon}, \tag{23}$$

where $\xi \in (0, h)$, so that partial differentiation with respect to x_2 transforms according to

$$\frac{\partial \bullet}{\partial x_2} = \frac{1}{\varepsilon} \frac{\partial \bullet}{\partial \xi}. \tag{24}$$

To leading-order, continuity of tractions $(22)_1$ yields

$$\varepsilon^{\zeta+1} \bar{\mu}^s \left. \frac{\partial u^s}{\partial x_2} \right|_{x_2=0} = \mu_2 \left. \frac{\partial u}{\partial \xi} \right|_{\xi=0}, \tag{25}$$

while continuity of displacements writes

$$u^s|_{x_2=0} = u|_{\xi=0}.$$

In terms of the scaled variable ξ, the equation of motion (19) in the layer becomes

$$\mu_1 \frac{\partial^2 u}{\partial x_1^2} + \mu_2 \frac{1}{\varepsilon^2} \frac{\partial^2 u}{\partial \xi^2} + \rho(x_1, \xi)\omega^2 u = 0, \tag{26}$$

so that, to leading-order, Eqs. (26), (25) and (21) become, respectively,

$$\frac{\partial^2 u}{\partial \xi^2} = 0 \quad (0<\xi<h), \quad \left.\frac{\partial u}{\partial \xi}\right|_{\xi=0} = 0, \quad \left.\frac{\partial u}{\partial \xi}\right|_{\xi=h} = 0. \tag{27}$$

The field equation $(27)_1$, together with boundary conditions $(27)_{2,3}$, implies that the leading-order approximation of u is independent of ξ, namely

$$u(x_1, \xi) \sim u^{(0)}(x_1) + \varepsilon^2 u^{(1)}(x_1, \xi). \tag{28}$$

The function $u^{(1)}(x_1, \xi)$ can be obtained after $u^{(0)}(x_1)$ is derived. The boundary-value problem for $u^{(1)}$ on the scaled cross-section $(0<\xi<h)$ may be derived by substituting Eq. (28) in Eq. (26)

$$\mu_2 \frac{\partial^2 u^{(1)}}{\partial \xi^2} + \mu_1 \frac{\mathrm{d}^2 u^{(0)}}{\mathrm{d}x_1^2} + \rho(x_1, \xi)\omega^2 u^{(0)} + O(\varepsilon^2) = 0 \quad (0<\xi<h) \tag{29}$$

and by substituting Eq. (28) into Eq. (25), with $\zeta = 1$ at the boundary Γ

$$\mu_2 \left.\frac{\partial u^{(1)}}{\partial \xi}\right|_{\xi=0} = \bar{\mu}^s \left.\frac{\partial u^s}{\partial x_2}\right|_{x_2=0}. \tag{30}$$

Taking into account that the boundary condition on the upper surface of the layer (21) requires

$$\left.\frac{\partial u^{(1)}}{\partial \xi}\right|_{\xi=h} = 0, \tag{31}$$

the solvability condition of differential equation (29), with the boundary conditions (30) and (31), is obtained by integrating Eq. (29) with respect to ξ between 0 and h, to obtain

$$h\mu_1 \frac{\mathrm{d}^2 u^{(0)}}{\mathrm{d}x_1^2} + h\hat{\rho}(x_1)\omega^2 u^{(0)} - \bar{\mu}^s \left.\frac{\partial u^s}{\partial x_2}\right|_{x_2=0} = 0, \tag{32}$$

where the average through-thickness density in the layer is

$$\hat{\rho}(x_1) = \frac{1}{h}\int_0^h \rho(x_1, \xi)\,\mathrm{d}\xi.$$

3.1. The response of the half space

The half space enters Eq. (32) through the last term on the left-hand side. The stiffness of the half space is assumed to be small, so that the problem can be asymptotically split into a Neumann boundary-value problem for the layer (see problem (27)) and a Dirichlet boundary-value problem for the half space. The last term on the left-hand side of Eq. (32) can now be evaluated by considering the problem of a free half space with negligibly small mass density subject to assigned displacements on the boundary. The field equation simply becomes Eq. (20), with $\rho^s = 0$ and $u^s = u$ on the surface, with solution

$$u^s(x_1, x_2) = -\frac{x_2}{\pi}\int_{-\infty}^{\infty} \frac{u^{(0)}(s)}{(x_1 - s)^2 + x_2^2}\,\mathrm{d}s. \tag{33}$$

The integral equation (33) provides the response of an isotropic elastic half space.

The derivative of Eq. (33) with respect to x_2, evaluated at $x_2 = 0$, can be used in Eq. (32) to give the integro-differential equation governing the time-harmonic behaviour of the layer

$$h\mu_1 \frac{\mathrm{d}^2 u^{(0)}}{\mathrm{d}x_1^2} + h\hat{\rho}(x_1)\omega^2 u^{(0)} + \frac{\bar{\mu}^s}{\pi} \Xint-_{-\infty}^{\infty} \frac{u^{(0)}(s)}{(x_1 - s)^2}\, \mathrm{d}s = 0. \tag{34}$$

3.1.1. The homogenous layer: harmonic response and displacement field

Eq. (34) is an integro-differential equation for the unknown function $u^{(0)}$. In the special case of a homogeneous layer (when the mass density is uniform, $\hat{\rho}(x_1) = \rho$) the solution for the layer and the half space is sought in the form of plane waves:

$$u^{(0)}(x_1) = U^{(0)} \mathrm{e}^{\mathrm{i}kx_1}, \tag{35}$$

where k is the wavenumber (positive and real), so that the integral becomes the Fourier transform of a known function, namely

$$\frac{U^{(0)}}{\pi} \Xint-_{-\infty}^{\infty} \frac{\mathrm{e}^{\mathrm{i}ks}}{(x_1 - s)^2}\, \mathrm{d}s = -U^{(0)}|k|\mathrm{e}^{\mathrm{i}kx_1},$$

and the integro-differential equation (34) leads to the characteristic equation

$$\bar{\omega}^2 = \frac{\bar{\mu}^s}{\mu_1} kh + (kh)^2, \tag{36}$$

where

$$\bar{\omega} = \omega h \sqrt{\frac{\rho}{\mu_1}}, \tag{37}$$

represents the dimensionless circular frequency. We note that the thickness of the layer h and the modulus $\bar{\mu}^s$ of the half space of the model problem (32) appear in the dimensionless circular frequency (37) and in Eq. (36).

A comparison between Eq. (36) and the exact dispersion curve (obtained numerically solving Eq. (A.2), see Appendix A) is possible by defining, for the latter, a non-dimensional frequency as that given by Eq. (37), but with the effective thickness εh replacing h. The result is plotted in Fig. 1a, where $\bar{k}$ corresponds to kh in Eq. (36) and to $k\varepsilon h$ in the exact analysis (reported in Appendix A).

Note that the exact solution allows incorporation of a non-null mass density in the half space, so that results for high contrast between the densities of the layer and half space have also been introduced in Fig. 1a ($\rho^s/\rho = 0.05$ has been chosen, representative of high-flexible electronic devices, as mentioned in the Introduction).

We note that Eq. (36) predicts an infinite group velocity (defined as $\mathrm{d}\omega/\mathrm{d}k$) at the origin. This is consistent with the hypothesis that the substrate has null mass density, $\rho^s = 0$. In the limit $\bar{k} \to 0$ the phase velocity ω/k approaches the shear wave speed of the half space that blows up for vanishing mass density, thus leading to infinite group velocity.

The second-order correction $u^{(1)}(x_1, \xi)$ of the displacement $u(x_1, \xi)$ can be evaluated by substituting Eqs. (35)–(37) into Eq. (29), with boundary conditions (30) and (31), thus obtaining

$$u^{(1)}(x_1, \xi) = -\frac{\bar{\mu}^s}{\mu_2} k\xi \left(\frac{\xi}{2h} - 1\right) U^{(0)} \mathrm{e}^{\mathrm{i}kx_1}.$$

Employing Eq. (23) to switch back from ξ to x_2 and the equality $\mu^s = \varepsilon\bar{\mu}^s$, the displacement field in the layer (28) is expressible as

$$u(x_1, x_2) = \left[1 - \frac{\mu^s}{\mu_2} \bar{k}\bar{x}_2 \left(\frac{\bar{x}_2}{2} - 1\right)\right] U^{(0)} \mathrm{e}^{\mathrm{i}kx_1}, \tag{38}$$

where $\bar{x}_2 = x_2/(\varepsilon h)$.

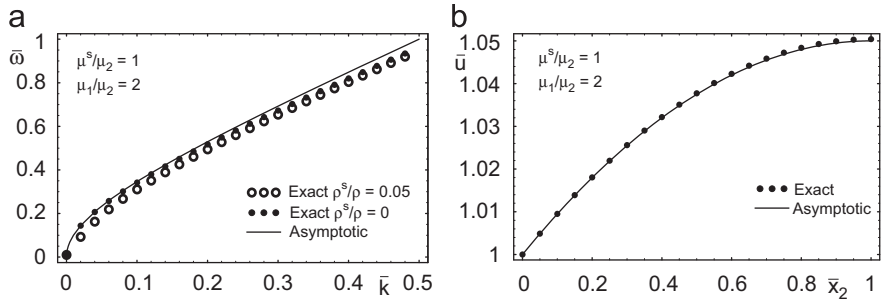

Fig. 1. Comparison between the exact numerical solution for Love waves propagating in a prestressed, orthotropic layer on an isotropic half space (Appendix A) and the long-wavelength closed-form approximation, Eqs. (36) and (38) ($\bar{k} = kh$ in Eqs. (36), (38); $\bar{k} = k\varepsilon h$ in Eqs. (A.2), (A.3)). Part (a): dimensionless circular frequency calculated through Eq. (A.2) (two cases are reported: null mass density of the half space, $\rho^s = 0$, and high contrast between the mass densities of the layer and the half space, $\rho^s/\rho = 0.05$) and calculated from the approximated, closed-form Eq. (36). Part (b): displacement field amplitude $\bar{u} = u/(U^{(0)}e^{ikx_1})$ across the layer thickness, for $\bar{k} = 0.1$, calculated through Eq. (A.3) (null mass density of the half space, $\rho^s = 0$, is only considered) and calculated from the approximated, closed-form Eq. (38).

Eq. (38) *represents a closed-form* (*but based on the simplifying long-wave assumption*) *solution for the propagation of Love waves at the interface between a prestressed*, *anisotropic layer resting on a soft*, *isotropic half space*. A closed-form solution such as Eq. (38) was previously not known even in the simple case of isotropic elasticity without prestress.

A comparison between the approximate solution (38) and the exact solution (known for isotropic elasticity without prestress, see e.g. Graff, 1975, and reported in Appendix A for anisotropic elasticity with prestress) is shown in Fig. 1b.

Fig. 1 shows that, for a half space with *vanishing mass density*, the asymptotic solution captures the long-wavelength vibration behaviour of the layer not only when the half space is less stiff than the layer, but also when the substrate has a shear modulus of the same order of that of the layer. Moreover, results in terms of displacements given by the closed-form solution (38) remain excellent even when the half space becomes much stiffer (50 times) than the layer. The calculations reported for $\rho^s/\rho = 0.05$ show that the asymptotic model with null mass density in the half space captures the dispersion behaviour with a small error (less than 10% for $\bar{k} = 0.1$), so that the analytical model developed in this article remains perfectly applicable to cases relevant in the design of MEMS.

3.1.2. The inhomogeneous layer and the cut-off interaction length

For an inhomogeneous layer, the solution cannot be expressed in the plane waves form (35), so that we have to go back to Eq. (34). We introduce now the hypothesis that at a point with longitudinal coordinate x_1 on the layer/half space interface Γ the displacement field $u^{(0)}$ depends on the interaction between the layer and the half space over a finite portion $(x_1 - d, x_1 + d)$ only, where d is a 'cut-off interaction length', assumed much smaller compared to $1/k$ and explicitly evaluated below for a homogeneous layer.

The Hadamard integral in Eq. (34) is now evaluated from $x_1 - d$ to $x_1 + d$

$$\frac{1}{\pi} \Xint= _{x_1-d}^{x_1+d} \frac{u^{(0)}(s)}{(x_1 - s)^2}\, \mathrm{d}s = -\frac{2}{\pi d} u^{(0)} + \frac{d}{\pi} \frac{\mathrm{d}^2 u^{(0)}}{\mathrm{d}x_1^2} + \text{ smaller terms.} \tag{39}$$

The equation governing anti-plane wave propagation in the layer then becomes

$$\left(1 + \frac{d}{\pi h}\right) \frac{\mathrm{d}^2 u^{(0)}}{\mathrm{d}x_1^2} + \left(\hat{\rho}(x_1) \frac{\omega^2}{\mu_1} - \frac{2}{\pi h d} \frac{\bar{\mu}^s}{\mu_1}\right) u^{(0)} = 0, \tag{40}$$

from which we can deduce that when d is sufficiently small, *the half space behaves as a bed of linear springs*, *with stiffness*

$$\bar{S}_a = \frac{2\bar{\mu}^s}{\pi h d}. \tag{41}$$

Restricting the attention to the homogeneous-layer solution, the interaction length d can be evaluated. In particular, a substitution of Eq. (35) into Eq. (40) yields

$$\bar{\omega}^2 = \frac{1}{\pi}\left(2\frac{\bar{\mu}^s h}{\mu_1 d} + k^2 h d\right) + (kh)^2. \tag{42}$$

Eqs. (36) and (42) provide non-dimensional frequency for anti-plane vibrations of a stiff layer bonded on a compliant substrate, under the hypothesis of large wavelength. Comparing these equations, an estimate of the interaction length d is obtained, entering Eq. (42) through the non-dimensional parameter kd

$$kd = \frac{\pi\bar{\mu}^s}{2\mu_1} \pm \frac{1}{2}\sqrt{\left(\pi\frac{\bar{\mu}^s}{\mu_1}\right)^2 - 8\frac{\bar{\mu}^s}{\mu_1}}, \tag{43}$$

which provides

(i) two real positive solutions if $\bar{\mu}^s/\mu_1 > 8/\pi^2$;
(ii) one real positive solution ($kd = 4/\pi$) if $\bar{\mu}^s/\mu_1 = 8/\pi^2$;
(iii) no real solutions if $\bar{\mu}^s/\mu_1 < 8/\pi^2$.

In the case (i), taking the two values of kd which satisfy Eq. (43), a perfect matching is obtained between the two solutions (42) and (36). However, if kd takes a value outside (inside) the interval between the two solutions defined by Eq. (43), Eq. (42) provides an overestimate (underestimate) of the circular frequency, which is correctly provided by the exact solution (36). For instance, when $\bar{\mu}^s/\mu_1 = 1$, Eq. (43) provides $kd = 0.887$ and $kd = 2.254$ and the maximum difference between the two values of $\bar{\omega}$ calculated from Eqs. (42) and (36) is less than $0.05\bar{\omega}$ for $kh = 0.1$. In the case (iii), no exact match is possible between Eqs. (42) and (36), however, the value $kd = \sqrt{2\bar{\mu}^s/\mu_1}$ minimizes the discrepancy between the two solutions for every kh. To illustrate this situation, we consider the values $\bar{\mu}^s/\mu_1 = 0.7$ and 0.5, and calculate $\bar{\omega}$ with an 'optimal' kd (respectively, equal to 1.183 and 1). Results are reported in Fig. 2, showing that the discrepancy is small, so that both approximations are good. The case (ii) is the transition between the two other cases and does not deserve detailed explanation.

We can conclude that in all the above-reported cases, an interaction length d exists, which provides an exact or excellent match between the spring model approximation (38) and the asymptotic solution.

Finally, it is worth noting that if only the first term in the series expansion (39) is employed, the interaction length matching Eqs. (36) and (42) can be calculated as

$$kd = 2/\pi,$$

which is the lower bound of the function (43) evaluated with the negative sign, so that the interaction length d is approximately one-tenth of the wavelength.

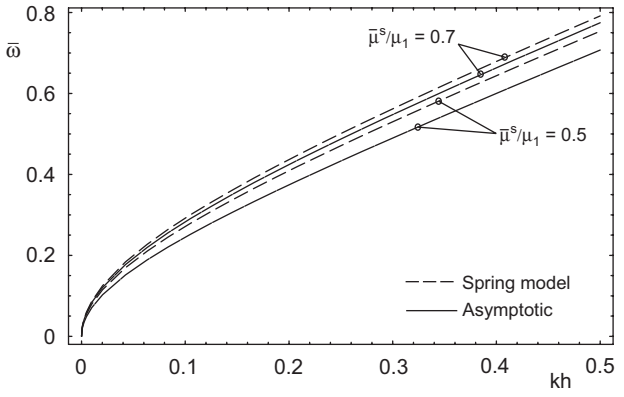

Fig. 2. Comparison between the dimensionless frequency $\bar{\omega}$ obtained from Eq. (36) (asymptotic analysis) and that obtained from Eq. (42) (so-called 'spring model') for $\bar{\mu}^s/\mu_1 = 0.7$ ($kd = 1.183$) and for $\bar{\mu}^s/\mu_1 = 0.5$ ($kd = 1$).

4. Plane-strain small-amplitude vibrations of a prestressed layer on a half space

We face now the problem of plane-strain vibrations of a prestressed, stiff layer lying on a compliant half space. The geometry is identical to that introduced in the previous section.

Within the layer we refer to a nonlinear elastic material homogeneously deformed in plane strain, for which the incremental constitutive law relating the incremental nominal stress tensor $\dot{t}_{ij}$ to the incremental displacement gradient $v_{i,j}$ are given by Eqs. (16). While we leave coefficients a, b and c free in these equations, we assume that the prestress appearing in the coefficients α, β and γ is small, that is

$$\alpha = \mu + \varepsilon^2\bar{\alpha}, \quad \beta = \mu + \varepsilon^2\bar{\beta}, \quad \gamma = \mu + \varepsilon^2\bar{\gamma}, \tag{44}$$

where

$$\bar{\alpha} = -\bar{\beta} = \frac{\bar{\sigma}_1 - \bar{\sigma}_2}{2}, \quad \bar{\gamma} = -\frac{\bar{\sigma}_1 + \bar{\sigma}_2}{2}. \tag{45}$$

The substrate is assumed to be 'soft', isotropic and without prestress, so that, from Eqs. (16), the relations between the components of the incremental nominal stress and the incremental displacement gradient take the form

$$\dot{t}^s_{11} = \varepsilon^3[(\bar{\lambda}^s + 2\bar{\mu}^s)v^s_{1,1} + \bar{\lambda}^s v^s_{2,2}], \quad \dot{t}^s_{22} = \varepsilon^3[\bar{\lambda}^s v^s_{1,1} + (\bar{\lambda}^s + 2\bar{\mu}^s)v^s_{2,2}], \tag{46}$$

$$\dot{t}^s_{12} = \dot{t}^s_{21} = \varepsilon^3\bar{\mu}^s(v^s_{2,1} + v^s_{1,2}),$$

where the Lamé moduli $\bar{\lambda}^s, \bar{\mu}^s$ are of the same order of the incremental moduli of the layer.

The material forming the layer is characterized by the mass density $\rho(x_1, x_2)$, while the inertia of the substrate is neglected ($\rho^s = 0$, as in the case of anti-plane vibrations, Section 3).

4.1. The long-wave asymptotic approximation

Taking into account that the flexural stiffness of the thin elastic body is much smaller compared to its longitudinal stiffness we write

$$v_1 = v_1\left(x_1, \frac{x_2}{\varepsilon}, t\right), \quad v_2 = v_2\left(x_1, \frac{x_2}{\varepsilon}, \varepsilon t\right),$$

and for the time-harmonic motion the differential equations with respect to v_1, v_2 follow. For the sake of convenience, we again introduce the scaled variable $\xi = \varepsilon^{-1}x_2$ so that Eq. (24) holds.

In terms of differential operators, the equations of motion in the layer are

$$\{\varepsilon^{-2}L_0 + \varepsilon^{-1}L_1 + L_2 + L_0^{\mathrm{ps}} + \varepsilon L_1^{\mathrm{ps}} + \varepsilon^2 L_2^{\mathrm{ps}}\}\boldsymbol{v} + \rho(x_1, \xi)\omega^2\begin{pmatrix} 1 & 0 \\ 0 & \varepsilon^2 \end{pmatrix}\boldsymbol{v} = \boldsymbol{0}, \tag{47}$$

where the superscript *ps* refers to terms depending on prestress and

$$L_0 = \begin{pmatrix} \mu & 0 \\ 0 & b \end{pmatrix}\frac{\partial^2}{\partial\xi^2}, \quad L_0^{\mathrm{ps}} = \begin{pmatrix} \bar{\beta} & 0 \\ 0 & 0 \end{pmatrix}\frac{\partial^2}{\partial\xi^2},$$

$$L_1 = \begin{pmatrix} 0 & c+\mu \\ c+\mu & 0 \end{pmatrix}\frac{\partial^2}{\partial\xi\,\partial x_1}, \quad L_1^{\mathrm{ps}} = \begin{pmatrix} 0 & \bar{\gamma} \\ \bar{\gamma} & 0 \end{pmatrix}\frac{\partial^2}{\partial\xi\,\partial x_1},$$

$$L_2 = \begin{pmatrix} a & 0 \\ 0 & \mu \end{pmatrix}\frac{\partial^2}{\partial x_1^2}, \quad L_2^{\mathrm{ps}} = \begin{pmatrix} 0 & 0 \\ 0 & \bar{\alpha} \end{pmatrix}\frac{\partial^2}{\partial x_1^2}, \tag{48}$$

while the operator of tractions is defined by

$$\begin{pmatrix} \dot{t}_{21}(\boldsymbol{v}) \\ \dot{t}_{22}(\boldsymbol{v}) \end{pmatrix} = \{\varepsilon^{-1}T_0 + T_1 + \varepsilon T_0^{\mathrm{ps}} + \varepsilon^2 T_1^{\mathrm{ps}}\}\boldsymbol{v}, \tag{49}$$

where

$$T_0 = \begin{pmatrix} \mu & 0 \\ 0 & b \end{pmatrix} \frac{\partial}{\partial \xi}, \quad T_0^{\mathrm{ps}} = \begin{pmatrix} \bar{\beta} & 0 \\ 0 & 0 \end{pmatrix} \frac{\partial}{\partial \xi}, \quad T_1 = \begin{pmatrix} 0 & \mu \\ c & 0 \end{pmatrix} \frac{\partial}{\partial x_1}, \quad T_1^{\mathrm{ps}} = \begin{pmatrix} 0 & \bar{\gamma} \\ 0 & 0 \end{pmatrix} \frac{\partial}{\partial x_1}.$$

It is assumed that

$$\begin{pmatrix} \dot{t}_{21}(\boldsymbol{v}) \\ \dot{t}_{22}(\boldsymbol{v}) \end{pmatrix} = \boldsymbol{0} \quad \text{as } \xi = h, \tag{50}$$

and that perfect contact conditions at the interface Γ between the layer and the substrate hold, imposing continuity of incremental displacements and nominal tractions

$$\boldsymbol{v}|_{\xi=0} = \boldsymbol{v}^s|_{x_2=0}, \quad \left.\begin{pmatrix} \dot{t}_{21}(\boldsymbol{v}) \\ \dot{t}_{22}(\boldsymbol{v}) \end{pmatrix}\right|_{\xi=0} = \left.\begin{pmatrix} \dot{t}^s_{21}(\boldsymbol{v}^s) \\ \dot{t}^s_{22}(\boldsymbol{v}^s) \end{pmatrix}\right|_{x_2=0}. \tag{51}$$

4.1.1. The asymptotic solution

It will be shown here that *the leading-order approximation of* $\boldsymbol{v}$ *in the stiff layer corresponds to the solution to the vibration problem of a prestressed beam on an elastic foundation*. Namely, the asymptotic ansatz of the displacement is

$$\boldsymbol{v} = \varepsilon^{-2} \begin{pmatrix} v_1^{(\mathrm{I},0)} \\ 0 \end{pmatrix} + \varepsilon^{-1} \boldsymbol{v}^{(\mathrm{I},1)} + \varepsilon^{-4} \begin{pmatrix} 0 \\ v_2^{(\mathrm{II},0)} \end{pmatrix} + \varepsilon^{-3} \boldsymbol{v}^{(\mathrm{II},1)} + \varepsilon^{-2} \boldsymbol{v}^{(\mathrm{II},2)} + \varepsilon^{-1} \boldsymbol{v}^{(\mathrm{II},3)} + \boldsymbol{V}, \tag{52}$$

where $v_1^{(\mathrm{I},0)} = v_1^{(\mathrm{I},0)}(x_1)$, $v_2^{(\mathrm{II},0)} = v_2^{(\mathrm{II},0)}(x_1)$. Note that $v_1^{(\mathrm{I},0)}(x_1)$ and $v_2^{(\mathrm{II},0)}(x_1)$ are the only functions in the asymptotic representation (52) with non-null mean value across the layer thickness. These functions, which will be derived later in this section, are the solutions of the following equations, governing axial and flexural vibrations of the layer and formally identical to the equations of a vibrating beam:

$$g \frac{\mathrm{d}^2 v_1^{(\mathrm{I},0)}}{\mathrm{d}x_1^2} + \hat{\rho}(x_1)\omega^2 v_1^{(\mathrm{I},0)} = 0, \tag{53}$$

$$-\frac{h^3}{12} g \frac{\mathrm{d}^4 v_2^{(\mathrm{II},0)}}{\mathrm{d}x_1^4} + h(\bar{\sigma}_1 - \bar{\sigma}_2) \frac{\mathrm{d}^2 v_2^{(\mathrm{II},0)}}{\mathrm{d}x_1^2} + h\hat{\rho}(x_1)\omega^2 v_2^{(\mathrm{II},0)} - R = 0, \tag{54}$$

where

$$g = a - \frac{c^2}{b}$$

reduces to the plane-strain elastic modulus $E/(1-\nu^2)$ for isotropic elasticity and, for a hyperelastic material with strain energy $\varphi(\lambda_1, \lambda_2, \lambda_3)$ is given by

$$g = \frac{\lambda_1}{\lambda_2} \left[\varphi_{,11} - \frac{(\varphi_{,12})^2}{\varphi_{,22}} \right],$$

where $\varphi_{,a} = \partial\varphi/\partial\lambda_a$. In Eq. (54) the average mass density $\hat{\rho}(x_1) = (1/h)\int_0^h \rho \, \mathrm{d}\xi$ also appears as well as the normal traction response of the elastic half space, R, defined in such a way that

$$\varepsilon^3 R = \dot{t}^s_{22}(x_1, 0) \tag{55}$$

when subjected (on its surface) to a prescribed vertical displacement $\{0, v_2^{(\mathrm{II},0)}\}$. In other words, the traction (55) is generated on the boundary of the half space as the solution of the problem

$$\boldsymbol{L}\boldsymbol{v}^{(0,s)} = \boldsymbol{0} \quad [x_1 \in (-\infty, +\infty), \quad x_2 < 0], \quad \boldsymbol{v}^{(0,s)} \longrightarrow \boldsymbol{0} \quad \text{as} \quad x_2 \longrightarrow -\infty \tag{56}$$

(where $L(\cdot)$ is the equilibrium differential operator) for which the boundary conditions

$$\boldsymbol{v}^{(0,s)} = \begin{pmatrix} 0 \\ v_2^{(\mathrm{II},0)}(x_1) \end{pmatrix} \quad \text{as } x_2 = 0, \;\; x_1 \in (-\infty, +\infty) \tag{57}$$

are prescribed. For a homogeneous layer, R can be given in closed-form, and the differential equation (54) explicitly solved, while, in general, we will provide integral expressions for it, which will be shown to reduce to a spring model when a certain cut-off distance for layer/half space transmission is introduced (Section 5.2).

Note that the half space does not enter Eq. (53), so that the asymptotic solution for longitudinal vibrations of the layer does not involve interactions with the half space, so that longitudinal vibrational characteristics depend only on the properties of the layer.

In general, the asymptotic model can be used as follows:

(i) The 'response' function R must be evaluated, depending on the problem at hand. Two situations will be explicitly considered in the following: the case when the layer is homogeneous (where a spring-type model is obtained, Eqs. (81) and (82)) and the case when it is not (where either a boundary integral equation, Eq. (91), or a spring-type model, Eq. (93), is obtained).
(ii) Eqs. (53) and (54) must be solved. This can be done explicitly in closed-form for a homogeneous layer. Otherwise, a numerical technique has to be used. In Section 7, for piecewise constant mass density, the dispersion equation is obtained through numerical solution of a characteristic equation derived from Bloch–Floquet technique.
(iii) Functions $\boldsymbol{v}^{(\mathrm{II},1)}$, $\boldsymbol{v}^{(\mathrm{II},2)}$, $\boldsymbol{v}^{(\mathrm{I},1)}$, $\boldsymbol{v}^{(\mathrm{II},3)}$, and $\boldsymbol{V}$ (appearing in representation (52)) must be obtained from Eqs. (62), (63), (69)–(72). These functions can be given in a closed-form for a homogeneous layer.

4.2. Derivation of the lower-dimensional model

In this section we describe an iterative formal algorithm for evaluation of the terms in the asymptotic expansion (52). We note that $\boldsymbol{v}^{(k,j)} = \boldsymbol{v}^{(k,j)}(x_1, \xi)$ inside the layer.

The asymptotic procedure consists of five steps; on each step we deal with a model boundary-value problem of the Neumann type on the scaled cross-section of the waveguide. The solvability conditions are verified at every step. In particular, Eqs. (53) and (54) will be obtained as the solvability conditions of the model problems that occur in the final iteration.

Step 1. The function $v_2^{(\mathrm{II},0)}$, describing the leading-order transverse displacement, satisfies the problem

$$\frac{\partial^2 v_2^{(\mathrm{II},0)}}{\partial \xi^2} = 0 \quad (0 < \xi < h), \quad \left.\frac{\partial v_2^{(\mathrm{II},0)}}{\partial \xi}\right|_{\xi=h} = 0, \quad \left.\frac{\partial v_2^{(\mathrm{II},0)}}{\partial \xi}\right|_{\xi=0} = 0,$$

and hence it is independent of ξ, that is,

$$v_2^{(\mathrm{II},0)} = v_2^{(\mathrm{II},0)}(x_1). \tag{58}$$

Step 2. For the vector function $\boldsymbol{v}^{(\mathrm{II},1)}$, we deduce

$$L_0 \boldsymbol{v}^{(\mathrm{II},1)} + L_1 \boldsymbol{v}^{(\mathrm{II},0)} = \boldsymbol{0} \quad (0 < \xi < h),$$

and note that $L_1 \boldsymbol{v}^{(\mathrm{II},0)} = \boldsymbol{0}$ due to condition (58) and the definition $(48)_1$. Hence,

$$\frac{\partial^2 \boldsymbol{v}^{(\mathrm{II},1)}}{\partial \xi^2} = \boldsymbol{0} \quad (0 < \xi < h), \tag{59}$$

and therefore $\boldsymbol{v}^{(\mathrm{II},1)}$ is linear in ξ. The boundary conditions (50) and (51) imply

$$T_0 \boldsymbol{v}^{(\mathrm{II},1)} + T_1 \boldsymbol{v}^{(\mathrm{II},0)} = \boldsymbol{0} \quad \text{as } \xi = 0 \quad \text{or} \quad \xi = h. \tag{60}$$

It is observed that the vibration problem of a stiff layer bonded to a soft half space splits asymptotically into a Neumann problem for the layer, where tractions are prescribed on the boundary, and a Dirichlet problem for the half space at the surface of which the displacements $\{0, v_2^{(\mathrm{II},0)}(x_1)\}$ are imposed, see problem (56).

Next, an integration of Eq. (59) shows that the vector function $\boldsymbol{v}^{(\mathrm{II},1)}$ can be represented in the form

$$\boldsymbol{v}^{(\mathrm{II},1)} = \boldsymbol{A}^{(\mathrm{II},1)}\xi + \boldsymbol{B}^{(\mathrm{II},1)}, \tag{61}$$

where vectors $\boldsymbol{A}^{(\mathrm{II},1)}$, $\boldsymbol{B}^{(\mathrm{II},1)}$ are chosen so that the condition (60) is satisfied. In particular, a substitution of Eq. (61) into Eq. (60) yields

$$\begin{pmatrix} \mu & 0 \\ 0 & b \end{pmatrix} \boldsymbol{A}^{(\mathrm{II},1)} + \begin{pmatrix} 0 & \mu \\ c & 0 \end{pmatrix} \begin{pmatrix} 0 \\ \dfrac{\mathrm{d}v_2^{(\mathrm{II},0)}}{\mathrm{d}x_1} \end{pmatrix} = \boldsymbol{0},$$

so that $\boldsymbol{A}^{(\mathrm{II},1)}$ results to be determined by

$$A_1^{(\mathrm{II},1)} = -\frac{\mathrm{d}v_2^{(\mathrm{II},0)}}{\mathrm{d}x_1}, \quad A_2^{(\mathrm{II},1)} = 0.$$

The vector $\boldsymbol{B}^{(\mathrm{II},1)}$ is chosen to provide a vanishing through-thickness average, namely $\int_0^h \boldsymbol{v}^{(\mathrm{II},1)}\,\mathrm{d}\xi = \boldsymbol{0}$, and hence

$$B_1^{(\mathrm{II},1)} = -A_1^{(\mathrm{II},1)}\frac{h}{2}, \quad B_2^{(\mathrm{II},1)} = 0.$$

Finally, the vector function $\boldsymbol{v}^{(\mathrm{II},1)}$ takes the form

$$\boldsymbol{v}^{(\mathrm{II},1)} = \begin{pmatrix} \left(\dfrac{h}{2} - \xi\right)\dfrac{\mathrm{d}v_2^{(\mathrm{II},0)}}{\mathrm{d}x_1} \\ 0 \end{pmatrix}. \tag{62}$$

Step 3. We proceed with the analysis of the terms $v_1^{(\mathrm{I},0)}$ and $\boldsymbol{v}^{(\mathrm{II},2)}$ of representation (52). Similarly to the Step 1 above, we deduce that

$$v_1^{(\mathrm{I},0)} = v_1^{(\mathrm{I},0)}(x_1),$$

therefore, for the vector function $\boldsymbol{v}^{(\mathrm{II},2)}$ the following boundary-value problem in the scaled cross-section $(0<\xi<h)$ holds:

$$L_0\boldsymbol{v}^{(\mathrm{II},2)} + L_1\boldsymbol{v}^{(\mathrm{II},1)} + L_2[v_2^{(\mathrm{II},0)}(x_1)\boldsymbol{e}_2] + L_0^{\mathrm{ps}}[v_2^{(\mathrm{II},0)}(x_1)\boldsymbol{e}_2] = \boldsymbol{0} \quad (0<\xi<h),$$

$$T_0\boldsymbol{v}^{(\mathrm{II},2)} + T_1\boldsymbol{v}^{(\mathrm{II},1)} = \boldsymbol{0} \quad \text{as } \xi = 0 \text{ or } \xi = h.$$

The solution of this problem, with zero average over the cross-section $(0<\xi<h)$ of the stiff layer, takes the form

$$\boldsymbol{v}^{(\mathrm{II},2)}(x_1,\xi) = \begin{pmatrix} 0 \\ \dfrac{c}{2b}\left[\left(\dfrac{h}{2} - \xi\right)^2 - \dfrac{h^2}{12}\right]\dfrac{\mathrm{d}^2 v_2^{(\mathrm{II},0)}}{\mathrm{d}x_1^2} \end{pmatrix}. \tag{63}$$

Step 4. At this stage, we analyse the terms $\boldsymbol{v}^{(\mathrm{I},1)}$ and $\boldsymbol{v}^{(\mathrm{II},3)}$ in the asymptotic ansatz (52). The corresponding governing equation is

$$L_0[\boldsymbol{v}^{(\mathrm{II},3)} + \boldsymbol{v}^{(\mathrm{I},1)}] + L_1[\boldsymbol{v}^{(\mathrm{II},2)} + v_1^{(\mathrm{I},0)}(x_1)\boldsymbol{e}_1] + L_2\boldsymbol{v}^{(\mathrm{II},1)} + L_0^{\mathrm{ps}}\boldsymbol{v}^{(\mathrm{II},1)} + L_1^{\mathrm{ps}}[v_2^{(\mathrm{II},0)}(x_1)\boldsymbol{e}_2] = \boldsymbol{0} \quad (0<\xi<h), \tag{64}$$

with boundary conditions

$$T_0[\boldsymbol{v}^{(\mathrm{II},3)} + \boldsymbol{v}^{(\mathrm{I},1)}] + T_1[\boldsymbol{v}^{(\mathrm{II},2)} + v_1^{(\mathrm{I},0)}(x_1)\boldsymbol{e}_1] + T_0^{\mathrm{ps}}\boldsymbol{v}^{(\mathrm{II},1)} + T_1^{\mathrm{ps}}[v_2^{(\mathrm{II},0)}(x_1)\boldsymbol{e}_2] = \boldsymbol{0} \quad \text{as } \xi = 0 \text{ or } \xi = h. \tag{65}$$

In our particular case

$$T_0^{\mathrm{ps}}\boldsymbol{v}^{(\mathrm{II},1)} + T_1^{\mathrm{ps}}[v_2^{(\mathrm{II},0)}\boldsymbol{e}_2] = -\bar{\sigma}_2\begin{pmatrix} \dfrac{\mathrm{d}v_2^{(\mathrm{II},0)}}{\mathrm{d}x_1} \\ 0 \end{pmatrix},$$

where we have employed the relationship $\bar{\gamma}-\bar{\beta}=-\bar{\sigma}_2$ (see Eqs. (45)). The functions $v_1^{(\mathrm{II},3)}$ and $v_2^{(\mathrm{I},1)}$ satisfy the following boundary-value problems on the scaled cross-section of the layer ($0<\xi<h$):

$$\frac{\partial^2 v_2^{(\mathrm{I},1)}}{\partial\xi^2}=0 \quad (0<\xi<h), \quad \left.\frac{\partial v_2^{(\mathrm{I},1)}}{\partial\xi}\right|_{\xi=h}=\left.\frac{\partial v_2^{(\mathrm{I},1)}}{\partial\xi}\right|_{\xi=0}=-\frac{c}{b}\frac{\mathrm{d}v_1^{(\mathrm{I},0)}}{\mathrm{d}x_1} \tag{66}$$

and

$$\frac{\partial^2 v_1^{(\mathrm{II},3)}}{\partial\xi^2}+\left(\frac{h}{2}-\xi\right)\left(\frac{g}{\mu}-\frac{c}{b}\right)\frac{\mathrm{d}^3 v_2^{(\mathrm{II},0)}}{\mathrm{d}x_1^3}=0 \quad (0<\xi<h), \tag{67}$$

$$\left.\frac{\partial v_1^{(\mathrm{II},3)}}{\partial\xi}\right|_{\xi=h}=\left.\frac{\partial v_1^{(\mathrm{II},3)}}{\partial\xi}\right|_{\xi=0}=-\frac{ch^2}{12b}\frac{\mathrm{d}^3 v_2^{(\mathrm{II},0)}}{\mathrm{d}x_1^3}+\frac{\bar{\sigma}_2}{\mu}\frac{\mathrm{d}v_2^{(\mathrm{II},0)}}{\mathrm{d}x_1}. \tag{68}$$

From Eqs. (64) and (65) we note that

$$v_2^{(\mathrm{II},3)}=0, \quad v_1^{(\mathrm{I},1)}=0.$$

Integration of Eq. $(66)_1$ with boundary conditions $(66)_{2,3}$ provides

$$v_2^{(\mathrm{I},1)}(x_1,\xi)=\frac{c}{b}\left(\frac{h}{2}-\xi\right)\frac{\mathrm{d}v_1^{(\mathrm{I},0)}}{\mathrm{d}x_1}, \tag{69}$$

whereas, for the function $v_1^{(\mathrm{II},3)}$, Eqs. (67) and (68) yield

$$v_1^{(\mathrm{II},3)}=\frac{\mathrm{d}^3 v_2^{(\mathrm{II},0)}}{\mathrm{d}x_1^3}\left\{-\frac{1}{6}\left(\frac{g}{\mu}-\frac{c}{b}\right)\left(\frac{h}{2}-\xi\right)^3+\left(\frac{h}{2}-\xi\right)\frac{h^2}{4}\left(\frac{g}{\mu}-\frac{c}{3b}\right)\right\}+\frac{\bar{\sigma}_2}{\mu}\left(\frac{h}{2}-\xi\right)\frac{\mathrm{d}v_2^{(\mathrm{II},0)}}{\mathrm{d}x_1}. \tag{70}$$

4.2.1. Solvability conditions (model problem for $\boldsymbol{V}$)

Substituting representation (52) into Eqs. (47), (50) and (51) we obtain a boundary-value problem in the variable $\boldsymbol{V}$. The field equations are

$$\mu\frac{\partial^2 V_1}{\partial\xi^2}+\left(g-\frac{\mu c}{b}\right)\frac{\mathrm{d}^2 v_1^{(\mathrm{I},0)}}{\mathrm{d}x_1^2}+\rho(x_1,\xi)\omega^2 v_1^{(\mathrm{I},0)}=0 \quad (0<\xi<h), \tag{71}$$

$$\begin{aligned} &b\frac{\partial^2 V_2}{\partial\xi^2}+(c+\mu)\frac{\partial^2 v_1^{(\mathrm{II},3)}}{\partial\xi\partial x_1}+\frac{\mu c}{2b}\left[\left(\frac{h}{2}-\xi\right)^2-\frac{h^2}{12}\right]\frac{\mathrm{d}^4 v_2^{(\mathrm{II},0)}}{\mathrm{d}x_1^4}\\ &\quad+\bar{\sigma}_1\frac{\mathrm{d}^2 v_2^{(\mathrm{II},0)}}{\mathrm{d}x_1^2}+\rho(x_1,\xi)\omega^2 v_2^{(\mathrm{II},0)}=0 \quad (0<\xi<h), \end{aligned} \tag{72}$$

where we have exploited the equation $\bar{\alpha}-\bar{\gamma}=\bar{\sigma}_1$ (see Eqs. (45)) and the function $v_1^{(\mathrm{II},3)}$ is given by Eq. (70). The boundary conditions for $\boldsymbol{V}$ are

$$\frac{\partial V_1}{\partial\xi}-\frac{ch}{2b}\frac{\mathrm{d}^2 v_1^{(\mathrm{I},0)}}{\mathrm{d}x_1^2}=0, \quad b\frac{\partial V_2}{\partial\xi}+c\frac{\partial v_1^{(\mathrm{II},3)}}{\partial x_1}=0 \quad \text{as } \xi=h, \tag{73}$$

$$\frac{\partial V_1}{\partial\xi}+\frac{ch}{2b}\frac{\mathrm{d}^2 v_1^{(\mathrm{I},0)}}{\mathrm{d}x_1^2}=0, \quad b\frac{\partial V_2}{\partial\xi}+c\frac{\partial v_1^{(\mathrm{II},3)}}{\partial x_1}=R(x_1) \quad \text{as } \xi=0, \tag{74}$$

where R is the normal response of the substrate, as introduced in Eq. (55).

The solvability conditions of differential equations (71) and (72) subject to the boundary conditions (73)–(74) can be written as

$$\int_0^h \left\{ \left(g - \frac{\mu c}{b}\right) \frac{\mathrm{d}^2 v_1^{(\mathrm{I},0)}}{\mathrm{d}x_1^2} + \rho(x_1,\xi)\omega^2 v_1^{(\mathrm{I},0)} \right\} \mathrm{d}\xi + \frac{\mu c h}{b} \frac{\mathrm{d}^2 v_1^{(\mathrm{I},0)}}{\mathrm{d}x_1^2} = 0 \tag{75}$$

for axial vibrations and

$$\int_0^h \left\{ (c+\mu) \frac{\partial^2 v_1^{(\mathrm{II},3)}}{\partial\xi \partial x_1} + \frac{\mu c}{2b} \left[\left(\frac{h}{2} - \xi\right)^2 - \frac{h^2}{12} \right] \frac{\mathrm{d}^4 v_2^{(\mathrm{II},0)}}{\mathrm{d}x_1^4} + \bar{\sigma}_1 \frac{\mathrm{d}^2 v_2^{(\mathrm{II},0)}}{\mathrm{d}x_1^2} + \rho(x_1,\xi)\omega^2 v_2^{(\mathrm{II},0)} \right\} \mathrm{d}\xi - c \left. \frac{\mathrm{d}v_1^{(\mathrm{II},3)}}{\mathrm{d}x_1} \right|_{\xi=h} + c \left. \frac{\mathrm{d}v_1^{(\mathrm{II},3)}}{\mathrm{d}x_1} \right|_{\xi=0} - R = 0 \tag{76}$$

for transversal vibrations of the layer. The substitution of Eq. (70) into Eqs. (75) and (76) leads to the differential equations (53) and (54) for axial and transversal vibrations.

5. Response of the substrate

In the asymptotic formulation, the response of the half space is 'condensed' in the response function R, Eq. (55). This function is separately derived in this section for the two cases of homogeneous (where a plane-wave solution is sufficient to capture the response) and inhomogeneous (i.e. with inhomogeneous mass density) layer for an orthotropic half space subject to a prestress state with principal directions aligned parallel to axes x_1, and x_2. For simplicity, the results will be finally particularized to incremental isotropic elasticity without prestress.

5.1. The case of the homogeneous layer: plane waves capture the solution

For a homogeneous layer, the solution in the half space is represented by plane waves. In particular, with reference to a *generic prestressed, orthotropic material*, Eqs. (16), the incremental displacement satisfying the equations of incremental equilibrium [$\rho = 0$ in Eqs. (18)] admits the representation

$$v_1^s = A_1 \mathrm{e}^{kr_1 x_2 + \mathrm{i}kx_1} + A_2 \mathrm{e}^{kr_2 x_2 + \mathrm{i}kx_1}, \quad v_2^s = -\mathrm{i}(c^s + \gamma^s) \left(A_1 \frac{r_1}{b^s r_1^2 - \alpha^s} \mathrm{e}^{kr_1 x_2} + A_2 \frac{r_2}{b^s r_2^2 - \alpha^s} \mathrm{e}^{kr_2 x_2} \right) \mathrm{e}^{\mathrm{i}kx_1}, \tag{77}$$

where A_1 and A_2 are constants and r_1 and r_2 are the solutions with positive real part of the characteristic equation

$$b^s \beta^s r^4 - [a^s b^s + \alpha^s \beta^s - (c^s + \gamma^s)^2] r^2 + a^s \alpha^s = 0. \tag{78}$$

For *isotropic elasticity*, in which $r = \pm 1$, the representation (77) is not valid. The new solution, which satisfies the Navier equations, is

$$v_1^s = \mathrm{i} \left[A_1 + A_2 \left(\frac{\lambda^s + 3\mu^s}{k(\lambda^s + \mu^s)} + x_2 \right) \right] \mathrm{e}^{\mathrm{i}kx_1 + kx_2}, \quad v_2^s = (A_1 + A_2 x_2) \mathrm{e}^{\mathrm{i}kx_1 + kx_2}.$$

Imposing the boundary conditions (57), namely $v_1^s(x_1,0) = 0$, $v_2^s(x_1,0) = v_2^{(\mathrm{II},0)}(x_1)$, we obtain $A_1 = -A_2$, so that Eq. $(77)_2$ at $x_2 = 0$ gives

$$v_2^{(\mathrm{II},0)}(x_1) = -\mathrm{i}A_1(c^s + \gamma^s) \left(\frac{r_1}{b^s r_1^2 - \alpha^s} + \frac{r_2}{b^s r_2^2 - \alpha^s} \right) \mathrm{e}^{\mathrm{i}kx_1}. \tag{79}$$

Taking the gradient of incremental displacement (77), with the help of Eq. (79), we obtain

$$v^s_{1,1} = -k(\mathrm{e}^{kr_1x_2} - \mathrm{e}^{kr_2x_2})\left(\frac{r_1(c^s+\gamma^s)}{b^s r_1^2-\alpha^s} + \frac{r_2(c^s+\gamma^s)}{b^s r_2^2-\alpha^s}\right)^{-1} v_2^{(\mathrm{II},0)}(x_1),$$

$$v^s_{2,2} = k\left(\frac{r_1^2}{b^s r_1^2-\alpha^s}\mathrm{e}^{kr_1x_2} + \frac{r_2^2}{b^s r_2^2-\alpha^s}\mathrm{e}^{kr_2x_2}\right)\left(\frac{r_1}{b^s r_1^2-\alpha^s} + \frac{r_2}{b^s r_2^2-\alpha^s}\right)^{-1} v_2^{(\mathrm{II},0)}(x_1), \tag{80}$$

and the traction at $x_2 = 0$ becomes

$$\dot{t}^s_{22} = kb^s \frac{r_1^2(b^s r_2^2-\alpha^s) + r_2^2(b^s r_1^2-\alpha^s)}{r_1(b^s r_2^2-\alpha^s) + r_2(b^s r_1^2-\alpha^s)} v_2^{(\mathrm{II},0)}(x_1), \tag{81}$$

representing *the incremental normal nominal traction at the surface of the half space as a function of the transversal incremental displacement*.

In the special case of linear isotropic elastic substrate without prestress, a similar procedure leads to the following expression of the incremental nominal traction at $x_2 = 0$:

$$\dot{t}^s_{22} = k\frac{2\mu^s(\lambda^s+2\mu^s)}{\lambda^s+3\mu^s} v_2^{(\mathrm{II},0)}(x_1). \tag{82}$$

5.1.1. Spring model for the elastic half space

Eq. (81) shows that the half space behaves as a bed of independent springs with transverse stiffness given by kS_t, where

$$S_t = b^s \frac{r_1^2(b^s r_2^2-\alpha^s) + r_2^2(b^s r_1^2-\alpha^s)}{r_1(b^s r_2^2-\alpha^s) + r_2(b^s r_1^2-\alpha^s)}. \tag{83}$$

Effects of prestress and orthotropy of the half space, which are now considered for the first time, are fully accounted for in Eq. (83). In the particular case of isotropic behaviour and null prestress, the stiffness can be obtained from Eq. (82) in the form

$$S_t = \frac{2(1-\nu^s)^2}{3-4\nu^s}\frac{E^s}{1-\nu^{s2}}, \tag{84}$$

in which the plane-strain elastic modulus $E^s/(1-\nu^{s2})$ has been written explicitly.

Referring to the problem of flexural vibrations of a layer, we can state that, coherently with the assumptions of Eqs. (46) and (55), the function R in Eq. (54) may be written as

$$R = \varepsilon^{-3}\dot{t}^s_{22} = k\bar{S}_t v_2^{(\mathrm{II},0)}(x_1), \tag{85}$$

where, according to Eq. (84),

$$\bar{S}_t = \frac{2(1-\nu^s)^2}{3-4\nu^s}\frac{\bar{E}^s}{1-\nu^{s2}}, \tag{86}$$

and $\bar{E}^s$ has the same order as the tangent modulus of the layer.

It is important to note that Eqs. (83) and (84) provide the stiffnesses of the bed of springs equivalent to the elastic half space as functions of the wavenumber k. This dependence also appears in other estimates known in the literature (Biot, 1937; Gough et al., 1940). Since these have been recently often used for analysing problems of engineering relevance (see for instance Karam and Gibson, 1995; Kardomateas, 2005; Wilder et al., 2006), we discuss this point in detail.

Biot (1937) has analysed a three-dimensional problem of quasi-static bending of a (finite-width) beam on an elastic half space subject to sinusoidal loading. A comparison with his results is not straightforward, however, to reproduce our results we have assumed an infinite width of the beam and $\Psi(\beta)/C = 1$. We have found that Biot's result coincides with Eq. (84), in the incompressible case, $\nu^s = 0.5$. Gough et al. (1940) extended the Biot approach to the study of the plane-strain buckling of a thin coating bonded to an elastic substrate, therefore

obtaining the following estimate for S_t:

$$S_t^{\text{Gough}} = \frac{2E^s}{(1+\nu^s)(3-\nu^s)}, \tag{87}$$

that differs from values (84) less than 25% for $\nu^s = 0.5$. The reason for the discrepancy is that Eq. (84) has been obtained by imposing null tangent displacement at the free surface of the half space, while Eq. (87) has been calculated assuming vanishing shear stress.

5.2. The integral representation and spring model for the response of the half space

In our asymptotic model the normal component of the displacement of the surface of the half space for flexural vibrations is prescribed to be equal to $v_2^{(\text{II},0)}$, while the parallel component is null, Eq. (57). In general, the displacements of the elastic half space are given by the integral equation

$$v_g^s(\boldsymbol{y}) = -\int_{-\infty}^{\infty} [t_2^{(g)}(\boldsymbol{x}-\boldsymbol{y}) v_2^{(\text{II},0)}(x_1)]_{x_2=0}\, \mathrm{d}x_1, \tag{88}$$

where $\boldsymbol{y}$ is an internal point of the half space and $t_2^{(g)}$ is the second component of the two-dimensional Green's function for tractions of the half space with null displacement on the boundary. Assuming for simplicity that the half space is made up of a linearly elastic isotropic material,[4] the function $t_2^{(g)}$ admits the representation

$$t_2^{(g)} = -\frac{1}{4\pi(1-\nu^s)} \frac{x_g - y_g}{|\boldsymbol{x}-\boldsymbol{y}|^2} \left(2\nu^s \delta_{1g} + 2(1-\nu^s)\delta_{2g} + 1 - 2\frac{(x_1-y_1)^2}{|\boldsymbol{x}-\boldsymbol{y}|^2} \right) + Q_2^{(g)}(\boldsymbol{x},\boldsymbol{y}),$$

where repeated indices are not summed, the singular terms are the same of the infinite body Green's function and $Q_2^{(g)}$ is a nonsingular term (Sheremet, 1984). Therefore, Eq. (88) becomes

$$v_g^s(\boldsymbol{y}) = \frac{1}{4\pi(1-\nu^s)} \int_{-\infty}^{\infty} \left[\frac{x_1\delta_{1g} - y_g}{(x_1-y_1)^2 + y_2^2} \left(2\nu^s\delta_{1g} + 2(1-\nu^s)\delta_{2g} + 1 - 2\frac{(x_1-y_1)^2}{(x_1-y_1)^2+y_2^2} \right) - Q_2^{(g)}(x_1,0;y_1,y_2) \right] v_2^{(\text{II},0)}(x_1)\, \mathrm{d}x_1. \tag{89}$$

Taking the gradient of Eq. (89) with respect to $\boldsymbol{y}$ and evaluating it at $y_2 = 0$ gives

$$v_{i,i}^s(y_1,0) = -\frac{1-2\nu^s}{4\pi(1-\nu^s)} \fint_{-\infty}^{\infty} \frac{v_2^{(\text{II},0)}(s)}{(s-y_1)^2}\, \mathrm{d}s - \int_{-\infty}^{\infty} \left. \frac{\partial Q_2^{(g)}(x_1,0;y_1,y_2)}{\partial y_i} \right|_{y_2=0} v_2^{(\text{II},0)}(x_1)\, \mathrm{d}x_1, \tag{90}$$

where repeated indices are not summed. The normal traction at $x_2 = 0$ can therefore be evaluated combining Eq. (90) with the constitutive equation of the substrate, i.e.

$$\dot{t}_{22}^s = \frac{E^s}{(1+\nu^s)(1-2\nu^s)} [\nu^s v_{1,1}^s + (1-\nu^s) v_{2,2}^s],$$

so that restricting the attention to the Hadamard integral in Eq. (90), we obtain

$$\dot{t}_{22}^s \sim -\frac{E^s}{4\pi(1-\nu^{s2})} \fint_{-\infty}^{\infty} \frac{v_2^{(\text{II},0)}(s)}{(s-y_1)^2}\, \mathrm{d}s. \tag{91}$$

As in the case of anti-plane motion and similarly to the cut-off distance usually introduced in the modelling of particle interactions calculated from Lennard-Jones potentials, we introduce now a 'cut-off interaction length' d, outside which the layer/half space interaction is neglected (this interaction length will later be explicitly evaluated for homogeneous layer). As a consequence, the Hadamard integral (91) can be reduced to

[4] Prestress and anisotropy can be accounted for in the way shown by Bigoni and Capuani (2002, 2005).

a Cauchy integral

$$\neq\!\!\!\!\!\int_{y_1-d}^{y_1+d} \frac{v_2^{(\mathrm{II},0)}(s)}{(s-y_1)^2}\,\mathrm{d}s = -\frac{2v_2^{(\mathrm{II},0)}(y_1)}{d} + \int_{y_1-d}^{y_1+d} \frac{v_2^{(\mathrm{II},0)}(s)-v_2^{(\mathrm{II},0)}(y_1)}{(s-y_1)^2}\,\mathrm{d}s. \tag{92}$$

In cases when the interaction length d is much smaller that $1/k$ the first term at the right-hand side of Eq. (92) becomes dominant and hence the incremental normal traction on the surface of the substrate can be approximated according to the formula

$$\dot{t}_{22}^{s} \sim \frac{E^s}{2d\pi(1-\nu^{s2})} v_2^{(\mathrm{II},0)}(y_1), \tag{93}$$

i.e. to this order of approximation the normal traction depends linearly on the imposed vertical displacement. Eq. (93) shows that *the half space behaves as a bed of springs even when the layer is inhomogeneous, provided an interaction length is introduced, which cuts-off the layer/half space transmission.*

6. The solution for a homogeneous layer and comparisons between the various approximations

It is shown in this section that the asymptotic solution of plane-strain vibrations of a (prestressed and orthotropic) layer on a soft half space can be solved in a closed-form, when the layer is assumed homogeneous. This solution will be compared to the exact solution (not available in a closed-form, given in Appendix B for completeness, and used in the examples under the assumption that coefficients in Eq. (6) are given by Eqs. (8)), to test the validity of the asymptotic approximation.

6.1. Closed-form asymptotic solution

For a homogeneous layer of constant density $\hat{\rho}(x_1)=\rho$, the solution of long-wavelength vibrations can be expressed in terms of plane waves. Then assuming the representation

$$v_1^{(\mathrm{I},0)} = w_1^{(\mathrm{I},0)} \mathrm{e}^{\mathrm{i}kx_1}, \quad v_2^{(\mathrm{II},0)} = w_2^{(\mathrm{II},0)} \mathrm{e}^{\mathrm{i}kx_1}, \tag{94}$$

the dispersion equation for axial vibrations can be easily obtained from Eq. (53) as

$$\omega = k\sqrt{\frac{g}{\rho}}, \tag{95}$$

showing that for longitudinal vibration of an infinite, free-standing beam the circular frequency is a linear function of the wavenumber.

On the other hand, the use of Eq. (81) (or Eq. (82)) in Eq. (54) provides the dispersion equation for bending vibrations, namely

$$\frac{\rho\omega^2 h^2}{g} = \frac{1}{12}(kh)^4 + \frac{\bar{\sigma}_1-\bar{\sigma}_2}{g}(kh)^2 + \frac{\bar{S}_t}{g}kh. \tag{96}$$

Eqs. (95) and (96), with the help of boundary conditions (73)–(74), may be used to solve Eqs. (71)–(72) in terms of the functions V_1 and V_2 appearing at zeroth-order in the asymptotic representation (52). The result is

$$V_1 = \frac{k^2 c}{2b}\,\xi(h-\xi) w_1^{(\mathrm{I},0)} \mathrm{e}^{\mathrm{i}kx_1},$$

$$V_2 = \left\{ \frac{k^2(c+\mu)}{2b}\left[\frac{k^2\eta_1}{32}(h-2\xi)^4 + \left(k^2h^2\eta_2 - \frac{\bar{\sigma}_2}{\mu}\right)(\xi-h)\xi\right] - \frac{k^4\mu c}{24b^2}\xi^2(h-\xi)^2 - \left(\frac{k^4h^2}{12}g - k^2\bar{\sigma}_2 + \frac{k\bar{S}_t}{h}\right)\frac{\xi^2}{2b} + G\xi \right\} w_2^{(\mathrm{II},0)} \mathrm{e}^{\mathrm{i}kx_1},$$

where

$$\eta_1 = -\frac{1}{6}\left(\frac{g}{\mu}-\frac{c}{b}\right), \quad \eta_2 = \frac{1}{4}\left(\frac{g}{\mu}-\frac{c}{3b}\right), \quad G = \frac{k^4h^3}{24b}g + \frac{k\bar{S}_t}{b} - \frac{k^2h\bar{\sigma}_2}{2b}.$$

Repeating now steps 2–4 of Section 4.2, we obtain the *closed-form representation of the asymptotic solution* (52) *for a homogeneous layer*. In particular, for pure axial vibrations we can take $w_2^{(\mathrm{II},0)} = 0$ and introduce the normalization $w_1^{(\mathrm{I},0)}/\varepsilon^2 = 1$, while for flexural vibrations $w_1^{(\mathrm{I},0)} = 0$ and $w_2^{(\mathrm{II},0)}/\varepsilon^4 = 1$. Therefore, for *axial vibrations* we obtain

$$v_1(x_1,x_2) = \left[1 + \frac{\bar{k}^2 c}{2b}\,\bar{x}_2(1-\bar{x}_2)\right]\mathrm{e}^{\mathrm{i}kx_1}, \quad v_2(x_1,x_2) = \mathrm{i}\bar{k}\frac{c}{b}\left(\frac{1}{2}-\bar{x}_2\right)\mathrm{e}^{\mathrm{i}kx_1}, \tag{97}$$

while for *flexural vibrations*

$$v_1(x_1,x_2) = \mathrm{i}\bar{k}\left(\frac{1}{2}-\bar{x}_2\right)\left[1 - \bar{k}^2\eta_1\left(\frac{1}{2}-\bar{x}_2\right)^2 - \bar{k}^2\eta_2 + \frac{\sigma_2}{\mu}\right]\mathrm{e}^{\mathrm{i}kx_1},$$

$$v_2(x_1,x_2) = \left\{1 - \bar{k}\frac{S_t}{2b}(\bar{x}_2-2)\bar{x}_2 - \frac{\bar{k}^2 c}{2b}\left[\left(\bar{x}_2-\frac{1}{2}\right)^2 - \frac{1}{12} + \frac{\sigma_2}{\mu}(\bar{x}_2-1)\bar{x}_2\right] + \frac{\bar{k}^4}{2b}\left[-\frac{g(\bar{x}_2-1)\bar{x}_2}{12}\right.\right.$$
$$\left.\left. + (c+\mu)\left(\frac{\bar{k}^2\eta_1}{32}(1-2\bar{x}_2)^4 + \eta_2(\bar{x}_2-1)\bar{x}_2\right) - \frac{\mu c(1-\bar{x}_2)^2\bar{x}_2^2}{12b}\right]\right\}\mathrm{e}^{\mathrm{i}kx_1}, \tag{98}$$

where the relationships $\varepsilon^3\bar{S}_t = S_t$ (see Eq. $(85)_2$) and $\varepsilon^2\bar{\sigma}_2 = \sigma_2$ (Eq. (45)) have been exploited and, as remarked in Section 4.1.1, the displacement fields v_1, v_2 associated with axial vibrations do not depend on the properties of the half space.

It is possible now to compare the asymptotic representations to the exact solution for an orthotropic, prestressed layer (reported in Appendix B), both in terms of dispersion equations and incremental displacement fields. To this end, Eq. (96) can be used to be compared to Eq. (B.7), in which the effective layer thickness εh must be employed in place of h. It is important to note that *the asymptotic analysis captures only the first two frequencies obtained from the numerical solution of Eq.* (B.7). *In particular, the first frequency corresponds to flexural vibrations of the layer, while the second frequency corresponds to axial vibrations of the layer*.

We focus the discussion on bending modes only. For the asymptotic approximation, Eq. (96) retains the main features of the model, namely, prestress and stiffness of the half space.

The comparison in terms of dispersion diagrams is reported in Fig. 3. In Fig. 3a, the half space is much softer than the layer ($E^s/g = 0.02$) and a relatively small tensile prestress is applied ($\sigma_1/g = 0.0077$). In this figure also the case of a non-null mass density of the half space is included (high contrast between the densities as in flexible electronics has been chosen, $\rho^s/\rho = 0.05$), which allows a judgment on the accuracy of our asymptotic model, employed beyond the situation of null mass density of the half space.

The agreement between the numerical and asymptotic solutions is excellent in the range of long-wavelengths ($\bar{k} < 0.6$–0.7). Moreover, in Fig. 3b it is shown that even when the stiffnesses of the two media are comparable, i.e. when $E^s/g = 1.5$ ($S_t/g = 0.897$) (and also for tensile longitudinal prestresses in the layer σ_1 on the order $0.1g$), the asymptotic solution captures the dispersion properties for long-wavelength flexural vibrations.

However, the mode shapes of the exact and the asymptotic analyses (Fig. 4) reveal that the latter method is accurate only for $E^s/g < 0.01$ and for the tensile prestress $\sigma_1 < 0.02g$ which is at the edge of the range of validity of the asymptotic method.

The dispersion diagram predicted by the closed-form asymptotic solution captures correctly the exact behaviour obtained numerically, even when the frequency diagram evidences a local minimum. The condition when this local minimum 'touches' the horizontal axis represents the layer bifurcation (or buckling) which, for the case under consideration, corresponds to a prestress $\sigma_{1,\mathrm{buckl}}/g = -0.048$ and a wavenumber $\bar{k} = 0.41$. These values may be calculated through the asymptotic approximation by imposing $\omega = 0$, so that Eq. (96) leads to the following evaluation of the bifurcation load and the critical wavenumber (found also by Gough

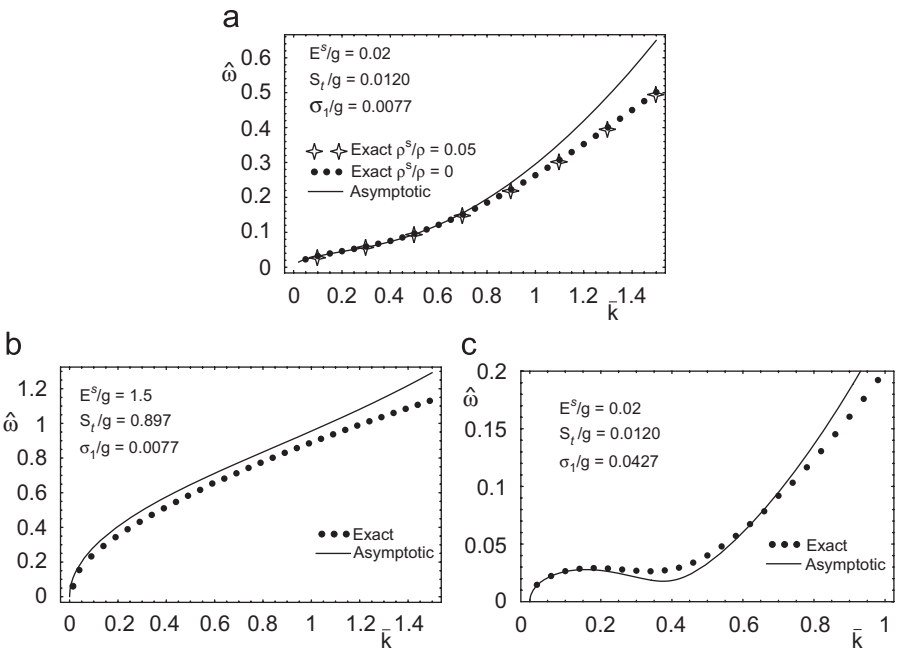

Fig. 3. Dimensionless frequency $\hat{\omega} = \omega h\sqrt{\rho/g}$ against the dimensionless wavenumber $\bar{k}$ for long-wavelength bending modes. Solid line: asymptotic, closed-form analysis, Eq. (96); black dots: lowest frequency obtained with the exact, numerical approach (Appendix B). Part (a): small prestress and small stiffness of the half space ($E^s/g = 0.02, \nu^s = 0.3, S_t/g = 0.0120, \sigma_1/g = 0.0077, \sigma_2 = 0$), a case of non-null mass density in the half space, $\rho^s/\rho = 0.05$, is also reported. Part (b): small prestress and stiffness of the half space comparable with that of the layer ($E^s/g = 1.5, \nu^s = 0.3, S_t/g = 0.897, \sigma_1/g = 0.0077, \sigma_2 = 0$). Part (c): prestress close to the buckling stress ($\sigma_{1,\mathrm{buckl}}/g = -0.048$) and small stiffness of the half space ($E^s/g = 0.02, \nu^s = 0.3, S_t/g = 0.0120, \sigma_1/g = -0.043, \sigma_2 = 0$).

et al., 1940, in the particular case of isotropic elasticity)

$$\left(\frac{\bar{\sigma}_1 - \bar{\sigma}_2}{g}\right)_{\mathrm{buckl}} = -0.825\left(\frac{\bar{S}_t}{g}\right)^{2/3}, \quad (kh)_{\mathrm{buckl}} = \left(6\frac{\bar{S}_t}{g}\right)^{1/3}. \tag{99}$$

It becomes clear from Eq. (99) that the layer is subject to a compressive stress very close to the bifurcation condition in Fig. 3c.

The fact emerging from Fig. 3c, that the dispersion curve is 'N-shaped', thus evidencing a negative group velocity zone, is connected to a dynamic instability. This feature is neither an artefact of the asymptotic analysis nor a consequence of the zero-mass assumption for the half space, since it is confirmed by numerical results obtained with the exact solution (in which a small, but non-null, mass density has been considered, namely, $\rho^s/\rho = 10^{-6}$). To substantiate this point, further results are shown in Fig. 5, relative to the same parameters used for Fig. 3c, except that now the prestress and the mass density are higher: $\sigma_1/g = -0.046$ and $\rho^s/\rho = 0.01$ for Fig. 5a, while $\rho^s/\rho = 0.1$ for Fig. 5b. The transition when the dispersion diagram becomes flat, corresponding to a zero group velocity, is characterized by a prestress value predicted by the asymptotic analysis equal to $\sigma_1/g = -0.0344$, while the exact approach provides $\sigma_1/g = -0.0385$.

6.2. Estimate of the interaction length

The substitution of Eq. (93) into Eq. (54) yields the spring-type approximation for bending vibrations for an elastic isotropic half space,

$$-\frac{h^3}{12}g\frac{\mathrm{d}^4 v_2^{(\mathrm{II},0)}}{\mathrm{d}x_1^4} + h(\bar{\sigma}_1 - \bar{\sigma}_2)\frac{\mathrm{d}^2 v_2^{(\mathrm{II},0)}}{\mathrm{d}x_1^2} + \left(h\hat{\rho}\omega^2 - \frac{\bar{E}^s}{2\pi\, d(1-\nu^{s2})}\right)v_2^{(\mathrm{II},0)} = 0, \tag{100}$$

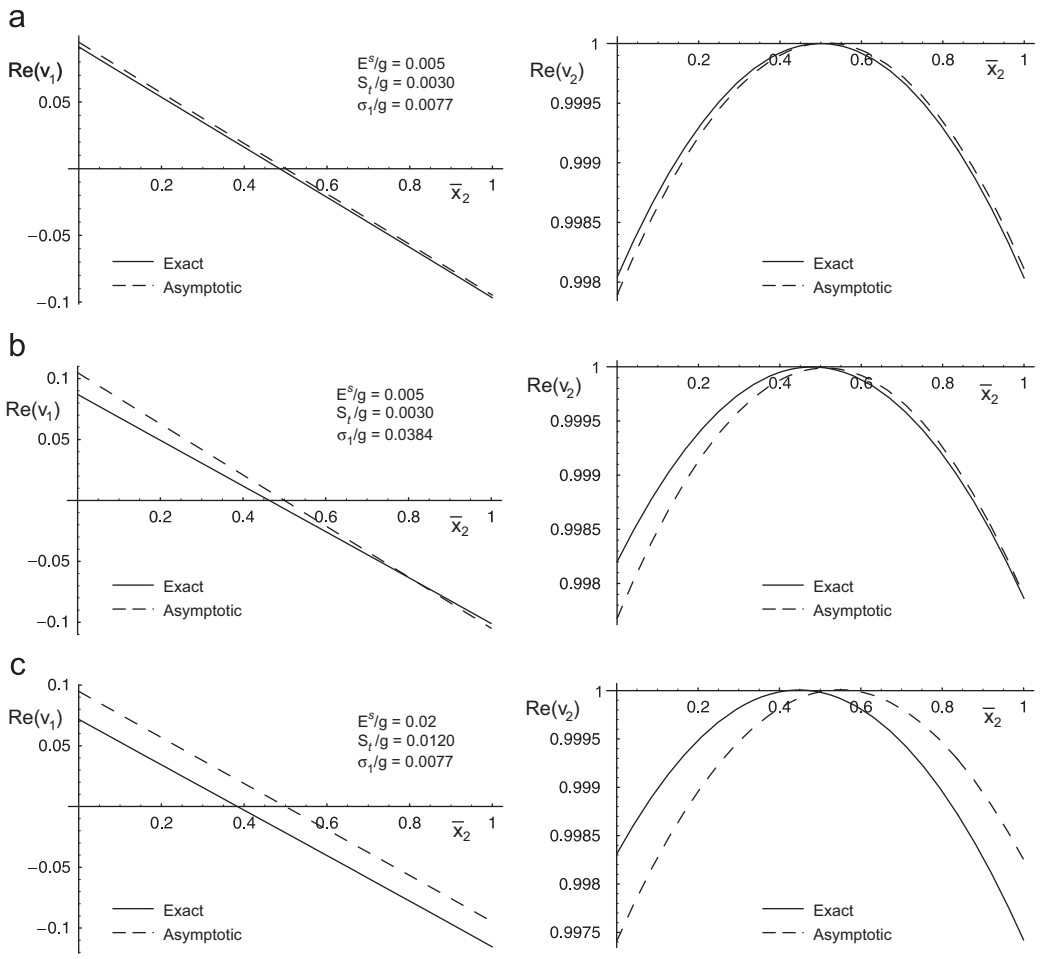

Fig. 4. Normalized displacement field of a flexural mode for $\bar{k} = 0.2$. Part (a): $E^s/g = 0.005, v^s = 0.3, S_t/g = 0.0030, \sigma_1/g = 0.0077, \sigma_2 = 0$. Part (b): $E^s/g = 0.005, v^s = 0.3, S_t/g = 0.0030, \sigma_1/g = 0.0384, \sigma_2 = 0$. Part (c): $E^s/g = 0.02, v^s = 0.3, S_t/g = 0.0120, \sigma_1/g = 0.0077, \sigma_2 = 0$. Solid line: exact, numerical approach (Appendix B); dashed line: asymptotic, closed-form analysis, Eq. (98).

which gives, in the case of a homogeneous layer $[\hat{\rho}(x_1) = \rho]$, the dispersion equation

$$\frac{\rho\omega^2 h^2}{g} = \frac{(kh)^4}{12} + (kh)^2 \frac{\bar{\sigma}_1 - \bar{\sigma}_2}{g} + \frac{\bar{E}^s h}{2\pi g\, d(1 - v^{s2})}. \tag{101}$$

The comparison between Eqs. (101) and (96), with $\bar{S}_t$ defined by Eq. (86), yields an estimate of the interaction length normalized through multiplication by the wavenumber k

$$kd = \frac{3 - 4v^s}{4\pi(1 - v^s)^2}. \tag{102}$$

Eq. (102) *provides an estimate of the interaction length d for flexural vibrations* that for $v^s = 0.3$ is about $\frac{1}{20}$ of the wavelength.

7. Band gaps are 'shifted' by the prestress in the layer

We consider in this section the dynamics of a stiff, thin elastic layer with periodic, piecewise constant mass density resting on a soft isotropic half space and, using the Bloch–Floquet analysis, we show that this system

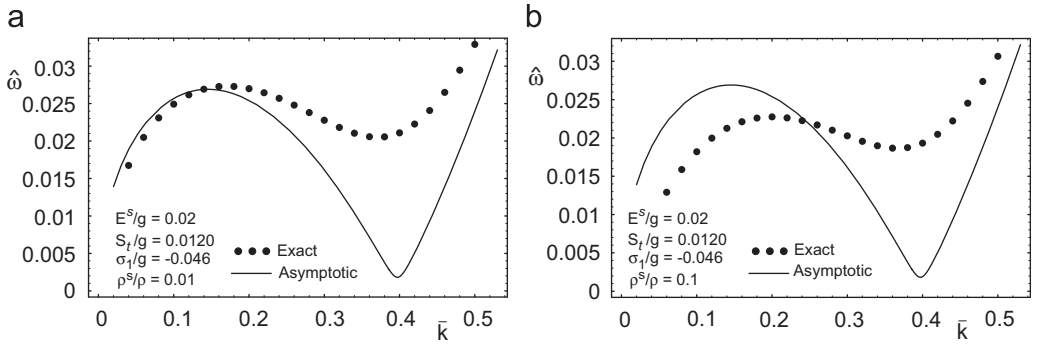

Fig. 5. Dimensionless frequency $\hat{\omega} = \omega h\sqrt{\rho/g}$ against the dimensionless wavenumber $\bar{k}$ for long-wavelength bending modes. Solid line: asymptotic, closed-form analysis, Eq. (96); black dots: lowest frequency obtained with the exact, numerical approach (Appendix B). Part (a): $E^s/g = 0.02, \nu^s = 0.3, S_t/g = 0.0120, \sigma_1/g = -0.046, \sigma_2 = 0, \rho^s/\rho = 0.01$. Part (b): $E^s/g = 0.02, \nu^s = 0.3, S_t/g = 0.0120, \sigma_1/g = -0.046, \sigma_2 = 0, \rho^s/\rho = 0.1$.

exhibits band gaps. We find that the prestress influences the dynamic properties of the system (a fact already known in homogeneous, prestressed materials, see Bigoni et al., 2007), but, more important, it influences the range of band gaps, so that, generally speaking, these are observed to 'shift' when prestress is changed. The result of this analysis is therefore that the prestress can be used as a tool to change with continuity the filtering properties of an elastic system, an effect never previously noticed.

We denote with h the thickness of the layer and we assume that the layer is periodic and composed of two parts taken for simplicity of equal length, l, so that the periodicity cell has length $2l$. The two parts have different, but constant, mass densities $\rho(x_1)$ and bending stiffnesses $h^3 g(x_1)/12$, so that $\rho(x_1) = \rho_1$, $g(x_1) = g_1$ if $(j-1)l < x_1 < jl$, $\rho(x_1) = \rho_2$, $g(x_1) = g_2$ if $jl < x_1 < (j+1)l$ ($j \in \mathbb{Z}$). The previously obtained asymptotic approximation (Section 4.1) is valid when the wavelength is large compared to the layer thickness h and *is on the same order of the length*, $2l$, *of the periodic cell*, so that the ratio h/l has to be small. Since the density is homogeneous in every sub-cell, the governing equations

$$-\frac{h^3}{12} g_m w_m'''' + h(\sigma_1 - \sigma_2) w_m'' + (h\rho_m \omega^2 - R_m) w_m = 0 \quad (m = 1, 2) \tag{103}$$

can be solved as in Section 6.1 with

$$w_m(x_1) = A_m \exp(\mathrm{i} k^{(m)} x_1) \quad (m = 1, 2),$$

and $R_m = k^{(m)} S$, with S given by Eq. (84). It turns out that the circular frequency satisfies the equation

$$(k^{(m)}h)^4 + \Sigma_m (k^{(m)}h)^2 + \bar{S}_m k^{(m)} h - P_m \omega^2 = 0 \quad (m = 1, 2), \tag{104}$$

where Σ_m ($m = 1, 2$) are the following dimensionless measures of the prestress:

$$\Sigma_m = \frac{12(\sigma_1 - \sigma_2)}{g_m} \quad (m = 1, 2), \tag{105}$$

while

$$\bar{S}_m = \frac{12S}{g_m}, \quad P_m = \frac{12\rho_m h^2}{g_m} \quad (m = 1, 2).$$

Eqs. (104) provide four solutions both for $k^{(1)}$ and $k^{(2)}$, so that the transverse displacements w_1, w_2 become linear combinations of four terms

$$w_1(x_1) = \sum_{p=1}^{4} A_1^p \exp(\mathrm{i} k_p^{(1)} x_1), \quad w_2(x_1) = \sum_{p=1}^{4} A_2^p \exp(\mathrm{i} k_p^{(2)} x_1).$$

The eight constants of the problem can be obtained by imposing continuity of displacement, rotation, bending moment and shear force at the interface between the two parts of the beam at $x_1 = 0$ (block $j = 0$):

$$w_1(0) = w_2(0), \quad w_1'(0) = w_2'(0), \quad g_1 w_1''(0) = g_2 w_2''(0), \quad g_1 w_1'''(0) = g_2 w_2'''(0). \tag{106}$$

The remaining four conditions follow from the quasi-periodicity condition:

$$\begin{aligned} &w_2(l^-) = w_1(-l^+)\exp(2\mathrm{i}Kl), \quad w_2'(l^-) = w_1'(-l^+)\exp(2\mathrm{i}Kl), \\ &g_2 w_2''(l^-) = g_1 w_1''(-l^+)\exp(2\mathrm{i}Kl), \quad g_2 w_2'''(l^-) = g_1 w_1'''(-l^+)\exp(2\mathrm{i}Kl), \end{aligned} \tag{107}$$

where K is the Bloch parameter ranging between $-\pi/(2l)$ and $\pi/(2l)$. Eqs. (106)–(107) provide a homogeneous system for the eight unknown constants A_1^p, A_2^p ($p = 1, \ldots, 4$). The vanishing of the determinant of the associated matrix yields the dispersion equation.

The dynamic properties of the system are illustrated in Fig. 6a–c, where the first branches of the dispersion equation are reported in Kl vs. $\sqrt{P_1}\omega$ diagrams. Focus is placed on the role of prestress $\sigma_1 - \sigma_2$, in particular, we have chosen $g_1 = g_2 = g$, so that $\Sigma_1 = \Sigma_2 = \Sigma$ and $\bar{S}_1 = \bar{S}_2 = \bar{S}$ (equal to 0.0001 in the simulations), and only the mass density is assumed to be a piecewise constant function of the longitudinal axis coordinate ($\rho_2/\rho_1 = 0.1$), therefore $P_2/P_1 = 0.1$. The remaining parameter, namely the ratio h/l, is taken to be 0.05.

In view of possible applications to 'flexible electronics' (see the Introduction), tensile prestresses in the layer are analysed (Fig. 6a, b), while prestress is taken to be zero in Fig. 6c. A compression state can be imposed to the system, but the slenderness of the layer and the high contrast between stiffnesses of the two materials leads to buckling instability, that in our case can be estimated through Eqs. $(99)_1$ and (105) as g is constant along the layer, providing $\Sigma_{\mathrm{buckl}} = -0.004$.

In each plot there are ranges of frequencies, the so-called 'band gaps', that correspond to non-propagating, decaying modes. These are highlighted with vertical black segments on the plots. Due to the linear dependence of the half space responses R_m on the wavenumber, the first branch always initiates at the origin of the diagram.

In Fig. 6d the band gap/pass band distribution is reported for different values of prestress for $0 < \sqrt{P_1}\omega < 0.3$. We note that, in general, an increase in the magnitude of the tensile stress leads to a shift of band gaps/pass bands towards higher frequencies and that this shift depends less than linearly on the prestress.

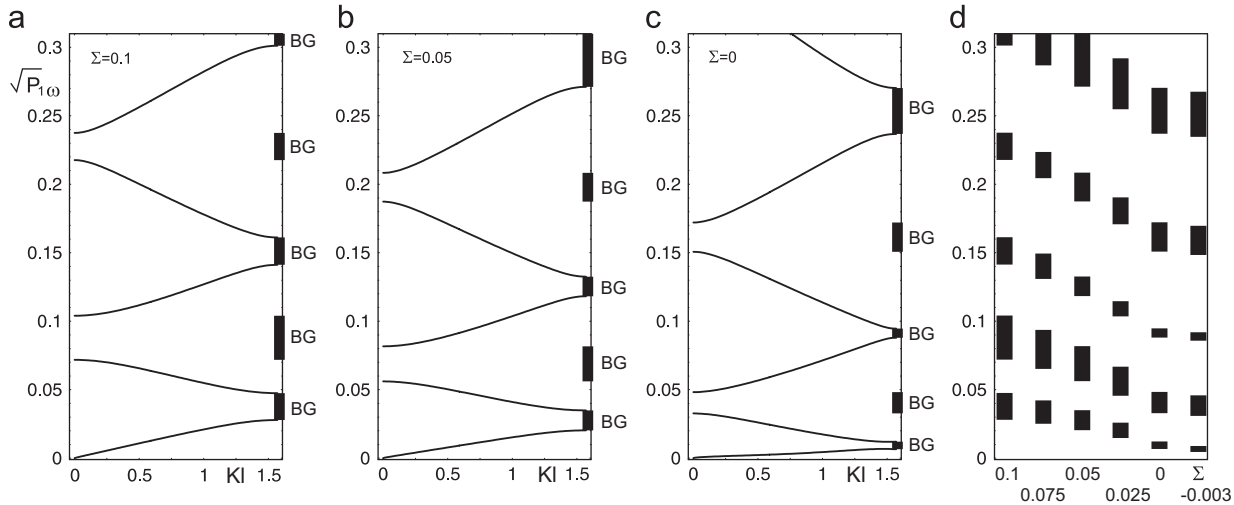

Fig. 6. Dispersion curves and band gap/pass band distribution for a thin, stiff layer on a soft elastic half space (becoming formally identical to a beam on an elastic foundation, Eq. (103), in the long-wave asymptotic representation) with piecewise constant mass density, $g_1 = g_2 = g$ ($P_2/P_1 = 0.1$, $\bar{S} = 0.0001$, $h/l = 0.05$). BG denotes a band gap. Parts (a), (b), (c): dispersion diagrams for three different values of axial prestress Σ (respectively, equal to 0.1, 0.05, 0). Part (d): band gap ranges vs. axial prestress Σ, evidencing the strong effect of prestress.

8. Conclusions

Long-wave asymptotics have been derived for time-harmonic, small-amplitude vibrations of an orthotropic, compressible and prestressed layer on an elastic half space (both under anti-plane shearing and plane-strain conditions). The half space has been assumed massless, isotropic elastic, and prestress free, assumptions that fit the mechanical properties of systems used in flexible electronics. When the layer is uniform, the solution is expressible in planar waves and 'spontaneously' leads to a new asymptotic, closed-form approximation in which the system is represented by a beam vibrating on a spring-like (or Winkler) foundation. For a inhomogeneous layer, the half space introduces a full nonlocality, which manifests itself in a hypersingular integral equation. It is shown that if the nonlocality is limited to a certain finite-size interaction zone, then the beam on spring-like foundation model is again recovered, with a new expression for the elastic spring constant. The performance of the different approximations is proven to be excellent by comparing to the homogeneous-layer solution, which is new and also reported.

The asymptotic analysis of the layer/half space system has permitted us investigation on the effects of the prestress on the dynamic properties of a periodic layer with piecewise constant properties. We have found a new effect, namely, that the prestress can be used as a parameter to change the forbidden frequencies of the mechanical system, a finding opening the way to new applications.

Acknowledgements

This research has been supported by a Marie Curie Transfer of Knowledge Grant of the European Community Sixth Framework Programme under contract number (MTKD-CT-2004-509809). Financial support of MIUR-PRIN 2005 (prot. 2005085973) and of the University of Trento are also acknowledged (D.B. and M.G.).

Appendix A. Exact solution for Love waves in a homogeneous prestressed anisotropic layer on a half space

The exact analysis of Love waves propagating parallel to the interface between a layer and a half space is based on the equations of motion (19) and (20), and boundary conditions (21)–(22). The solution in terms of displacement in the two domains is

$$u = (B_1 \mathrm{e}^{kqx_2} + B_2 \mathrm{e}^{-kqx_2})\mathrm{e}^{\mathrm{i}kx_1}, \quad u^s = B^s \mathrm{e}^{kq^s x_2 + \mathrm{i}kx_1}, \tag{A.1}$$

where

$$q = \sqrt{\frac{\mu_1}{\mu_2} - \frac{\rho\omega^2}{k^2\mu_2}}, \quad q^s = \sqrt{1 - \frac{\rho^s\omega^2}{k^2\mu^s}},$$

and B_1, B_2, B^s are three coefficients to be determined imposing boundary conditions. To impose the decay of the solution in the half space, we require that $\mathrm{Re}(q^s) > 0$.

Nontrivial solution of Eqs. (21) and (22) implies the vanishing of the determinant of the coefficient matrix, leading to the characteristic equation of the problem

$$\sqrt{\mu^s\left(\mu^s - \frac{\rho^s\omega^2}{k^2}\right)} + \sqrt{\mu_2\left(\mu_1 - \frac{\rho\omega^2}{k^2}\right)} \tanh\left[k\varepsilon h\sqrt{\frac{\mu_1}{\mu_2} - \frac{\rho\omega^2}{\mu_2 k^2}}\right] = 0, \tag{A.2}$$

where εh is the layer thickness. Eq. (A.2) can be numerically solved for fixed values of non-dimensional wavenumber $k\varepsilon h$ to yield the circular frequency ω. Finally, Eqs. (21) and (22) allow us to express B_2 and B^s in terms of B_1, so that the displacements in Eq. (A.1) take the form

$$u = B_1[\mathrm{e}^{kqx_2} + \mathrm{e}^{2k\varepsilon hq}\mathrm{e}^{-kqx_2}]\ \mathrm{e}^{\mathrm{i}kx_1}, \quad u^s = B_1[1 + \mathrm{e}^{2k\varepsilon hq}]\ \mathrm{e}^{kq^s x_2 + \mathrm{i}kx_1}. \tag{A.3}$$

Appendix B. Exact solution for plane-strain time-harmonic vibrations of a homogeneous prestressed anisotropic layer on a half space

In-plane harmonic solutions to the equations of motion

$$\dot{t}_{11,1}+\dot{t}_{21,2}=\rho v_{1,tt},\quad \dot{t}_{12,1}+\dot{t}_{22,2}=\rho v_{2,tt}, \tag{B.1}$$

$$\dot{t}^s_{11,1}+\dot{t}^s_{21,2}=\rho^s v^s_{1,tt},\quad \dot{t}^s_{12,1}+\dot{t}^s_{22,2}=\rho^s v^s_{2,tt} \tag{B.2}$$

are sought, satisfying the boundary conditions

$$\dot{t}_{22}=\dot{t}_{21}=0 \quad \text{as } x_2=\varepsilon h, \tag{B.3}$$

$$\dot{t}_{22}=\dot{t}^s_{22},\quad \dot{t}_{21}=\dot{t}^s_{21},\quad v_1=v^s_1,\quad v_2=v^s_2 \quad \text{as } x_2=0. \tag{B.4}$$

The displacement field in the two media, solving Eqs. (B.1)–(B.4), is

$$v_j=(A^j_1 e^{ks_1x_2}+A^j_2 e^{ks_2x_2}+A^j_3 e^{-ks_1x_2}+A^j_4 e^{-ks_2x_2})e^{i(kx_1-\omega t)} \quad (j=1,2) \tag{B.5}$$

for the layer, and

$$v^s_j=(C^j_1 e^{kr_1x_2}+C^j_2 e^{kr_2x_2})e^{i(kx_1-\omega t)} \quad (j=1,2) \tag{B.6}$$

for the half space. In Eq. (B.5) coefficients $\pm s_1, \pm s_2$ satisfy the characteristic equation

$$b\beta s^4-[ab+\alpha\beta-(c+\gamma)^2]s^2+a\alpha=0,$$

whereas in Eq. (B.6) r_1, r_2 are the solutions of Eq. (78) with positive real parts. The problem involves twelve constants that will be reduced to six, determined by the boundary conditions. In fact, the insertion of Eqs. (B.5) and (B.6), respectively, in Eqs. $(B.1)_1$ and $(B.2)_1$ yields

$$A^2_m=i\frac{s_m^2\beta-a+\rho\omega^2/k^2}{s_m(c+\gamma)}A^1_m \quad (m=1,\ldots,4; s_3=-s_1, s_4=-s_2),$$

$$C^2_m=i\frac{r_m^2\beta^s-a^s+\rho^s\omega^2/k^2}{r_m(c^s+\gamma^s)}C^1_m \quad (m=1,2).$$

The six unknowns can be collected in the vector $[a]^T=[A^1_1\ A^1_2\ A^1_3\ A^1_4\ C^1_1\ C^1_2]$, so that the system of boundary conditions (B.3)–(B.4) may be formally expressed in the form

$$[M][a]=[0],$$

where $[M]$ is a 6×6 matrix which depends on the properties of the two media, on k and on the eigenvalue ω. Once having fixed k, the dispersion equation simply becomes

$$\det[M(\omega)]=0, \tag{B.7}$$

which can be numerically solved to obtain the circular frequency ω.

The results described in Section 6.1 have been presented for a prestressed, incrementally isotropic layer obeying Eq. (5), with coefficients e_j $(j=1,\ldots,9)$ and moduli $a,b,c,\alpha,\beta,\gamma$ given by Eqs. (8) and (17), respectively. The half space has been taken with a small mass density ρ^s, unstressed and isotropic, so that the half space incremental moduli are

$$a^s=b^s=\lambda^s+2\mu^s,\quad c^s=\lambda^s,\quad \alpha^s=\beta^s=\gamma^s=\mu^s.$$

References

Bigoni, D., Capuani, D., 2002. Green's function for incremental nonlinear elasticity: shear bands and boundary integral formulation. J. Mech. Phys. Solids 50, 471–500.

Bigoni, D., Capuani, D., 2005. Time-harmonic Green's function and boundary integral formulation for incremental nonlinear elasticity: dynamics of wave patterns and shear bands. J. Mech. Phys. Solids 53, 1163–1187.

Bigoni, D., Movchan, A.B., 2002. Statics and dynamics of structural interfaces in elasticity. Int. J. Solids Struct. 39, 4843–4865.
Bigoni, D., Ortiz, M., Needleman, A., 1997. Effect of interfacial compliance on bifurcation of a layer bonded to a substrate. Int. J. Solids Struct. 34, 4305–4326.
Bigoni, D., Capuani, D., Bonetti, P., Colli, S., 2007. A novel boundary element approach to time-harmonic dynamics of incremental nonlinear elasticity: the role of pre-stress on structural vibrations and dynamic shear banding. Comput. Methods Appl. Mech. Eng. 196, 4222–4249.
Biot, M.A., 1937. Bending of an infinite beam on an elastic foundation. J. Appl. Mech. 59, A1–A7.
Cai, Z.X., Fu, Y.B., 2000. Exact and asymptotic stability analyses of a coated elastic half space. Int. J. Solids Struct. 37, 3101–3119.
Cimpoiasu, A., van der Pers, N.M., de Keyser, T.H., Venema, A., Vellekoop, E.J., 1996. Stress control of piezoelectric ZnO films on silicon substrates. Smart Mater. Struct. 5, 744–750.
Gei, M., 2008. Elastic waves guided by a material interface. Eur. J. Mech. A/Solids, in press, doi:10.1016/j.euromechsol.2007.10.002.
Gei, M., Ogden, R.W., 2002. Vibration of a surface-coated elastic block subject to bending. Math. Mech. Solids 7, 607–628.
Gei, M., Bigoni, D., Franceschini, G., 2004. Thermoelastic small-amplitude wave propagation in nonlinear elastic multilayers. Math. Mech. Solids 9, 555–568.
Gough, G.S., Elam, C.F., de Bruyne, N.A., 1940. The stabilisation of a thin sheet by a continuous supporting medium. J. R. Aero. Soc. 44, 12–13.
Graff, K.F., 1975. Wave Motion in Elastic Solids. Oxford University Press, Cambridge, MA.
Gray, D.S., Tien, J., Chen, C.S., 2004. High-conductivity elastomeric electronics. Adv. Mater. 16, 393–397.
Guenneau, S., Movchan, A.B., 2004. Analysis of elastic band structures for oblique incidence. Arch. Ration. Mech. Anal. 171, 129–150.
Gurtin, M.E., Murdoch, A.I., 1975. A continuum theory of elastic material surfaces. Arch. Ration. Mech. Anal. 57, 291–323.
Hill, R., 1979. On the theory of plane strain in finitely deformed compressible materials. Math. Proc. Camb. Philos. Soc. 86, 161–178.
Karam, G.N., Gibson, L.J., 1995. Elastic buckling of cylindrical shells with elastic cores. 1. Analysis. Int. J. Solids Struct. 32, 1259–1283.
Kardomateas, G.A., 2005. Wrinkling of wide sandwich panels/beams with orthotropic phases by an elasticity approach. J. Appl. Mech. 72, 818–825.
Li, T., Huang, Z., Suo, Z., Lacour, S.P., Wagner, S., 2004. Stretchability of thin metal films on elastomer substrates. Appl. Phys. Lett. 85, 3435–3437.
Lian, L., Sottos, N.R., 2004. Stress effects in sol–gel derived ferroelectric thin films. J. Appl. Phys. 95, 629–634.
Mead, D.J., 2002. Free-vibrations of self-strained assemblies of beams. J. Sound Vib. 249, 101–127.
Ogden, R.W., Steigmann, D.J., 2002. Plane strain dynamics of elastic solids with intrinsic boundary elasticity, with application to surface wave propagation. J. Mech. Phys. Solids 50, 1869–1896.
Platts, S.B., Movchan, N.V., McPhedran, R.C., Movchan, A.B., 2003. Band gaps and elastic waves in disordered stacks: normal incidence. Proc. R. Soc. London A 459, 221–240.
Sheremet, V.D., 1984. Static equilibrium of elastic half-plane under concentrated force. Prikl. Mekh. 20, 80–88.
Steigmann, D.J., Ogden, R.W., 1997. Plane deformations of elastic solids with intrinsic boundary elasticity. Proc. R. Soc. London A 455, 437–474.
Steigmann, D.J., Ogden, R.W., 1999. Elastic surface–substrate interactions. Proc. R. Soc. London A 453, 853–877.
Wang, C.C., 1970. A new representation theorem for isotropic functions, parts I and II. Arch. Ration. Mech. Anal. 36, 166–223.
Wilder, E.A., Guo, S., Lin-Gibson, S., Fasolka, M.J., Stafford, C.M., 2006. Measuring the modulus of soft polymer networks via a buckling-based metrology. Macromolecules 39, 4138–4143.
Zamir, E.A., Taber, L.A., 2004. On the effects of residual stress in microindentation tests of soft tissue structures. J. Biomech. Eng. ASME 126, 276–283.